Chemical Science

ROYAL SOCIETY OF CHEMISTRY

PERSPECTIVE

View Article Online
View Journal | View Issue

Cite this: *Chem. Sci.*, 2022, **13**, 8224

All publication charges for this article have been paid for by the Royal Society of Chemistry

Received 14th May 2022
Accepted 20th June 2022

DOI: 10.1039/d2sc02706b

rsc.li/chemical-science

Engendering reactivity at group 5-heteroatom multiple bonds *via* π-loading

Jade I. Fostvedt,[a] Jocelyne Mendoza,[a] Sacy Lopez-Flores,[b] Diego Alcantar,[a] Robert G. Bergman *[a] and John Arnold *[a]

In this Perspective, we discuss the strategy of π-loading, *i.e.*, coordination of two or more strongly π-donating ligands to a single metal center, as it applies to promoting reactivity at group 5 transition metal-imido groups. When multiple π-donor ligands compete to interact with the same symmetrically-available metal d_π orbitals, the energy of the imido-based frontier molecular orbitals increases, leading to amplified imido-based reactivity. This strategy is of particular relevance to group 5 metals, as mono(imido) complexes of these metals tend to be inert at the imido group. Electronic structure studies of group 5 bis(imido) complexes are presented, and examples of catalytically and stoichiometrically active group 5 bis(imido) and chalcogenido–imido complexes are reviewed. These examples are intended to encourage future work exploring π-loaded bis(imido) systems of the group 5 triad.

1. Introduction

Imido complexes of early transition metals (groups 3–5) are key intermediates in the stoichiometric and catalytic syntheses of many nitrogen-containing organic compounds, such as pyrroles, carbodiimides, amines, imines, and guanidines.[1,2] These transformations are mediated by elementary reactions of small molecule substrates with the metal–imido bond, primarily 1,2-additions of element–hydrogen bonds,[3–5] [2 + 2] cycloadditions with unsaturated substrates,[2,6,7] and imido group transfer.[8] Early transition metal–imido complexes first gained attention for their remarkable reactivity in 1988, when both Wolczanski and Bergman reported the seminal examples of Zr imido-mediated C–H activation.[9,10]

Since then, the chemistry of group 3 and 4 mono(imido) complexes has expanded rapidly,[5,6,11–23] while the related chemistry of group 5 mono(imido) complexes has comparatively lagged.[24–28] This discrepancy can be attributed to the increasing covalency of the bonding interaction between the group 5 metal nd and the imido 2p orbitals, relative to the more polar and reactive bonds formed between imido ligands and transition metals of groups 3 and 4.[29,30] To address this issue, our group and others have employed a π-loading strategy to enhance reactivity at group 5 metal–imido bonds. This strategy involves coordination of two or more strongly π-bonding ligands (*i.e.*, imido, oxo, nitrido, *etc.*; see Fig. 1 for depictions of

[a]*Department of Chemistry, University of California, Berkeley, CA, 94720, USA. E-mail: arnold@berkeley.edu; rbergman@berkeley.edu*

[b]*College of Letters & Science, University of California, Berkeley, CA, 94720, USA*

Jade I. Fostvedt is a recent graduate of the University of California, Berkeley (PhD with Prof. John Arnold, 2022), and previously received her B.S. in chemistry from the University of South Dakota (2017). Her current research interests include design of tantalum systems for small molecule activation, as well as implementation and assessment of programs to promote equity among incoming undergraduate students in chemistry. She has a particular passion for teaching inorganic chemistry.

Jocelyne Mendoza is currently an undergraduate in the College of Chemistry at the University of California, Berkeley. She is interested in the synthesis of organic compounds for production of therapeutic methods and drugs, along with contributing to diversity efforts in the field of chemistry.

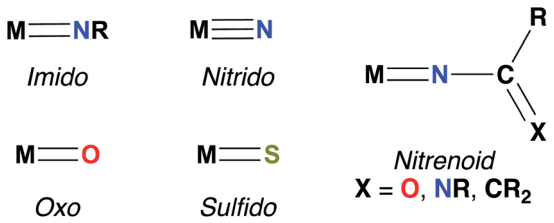

Fig. 1 Common π-bonded metal-heteroatom species.

common π-bonding ligands.) to a single metal center; these ligands compete to interact with the symmetrically available d_π orbitals on the metal center, destabilizing and polarizing metal-imido groups and thus engendering imido-based reactivity.[29–32] The π-loading strategy has found great utility in the realm of early transition metal imido chemistry, in particular through combinations of an imido group and the orbitally related cyclopentadienyl (Cp) ligand.[9,14,24,25,33,34]

The π-loading strategy has proven particularly successful in expanding imido-based reactivity in group 5 bis(imido) transition metal complexes, relative to their unreactive mono(imido) congeners.[29,30] In this Perspective, we communicate how to implement π-loading to increase reactivity at group 5 transition metal–imido bonds, as well as highlight how these design principles can be extended to other π-donor ligands, such as oxos and sulfidos. This Perspective is organized as follows: we first detail the electronic structure of bis(imido) complexes, and outline synthetic routes to bis(imido) complexes. Second, we present examples of reactive π-loaded bis(imido) complexes and emerging research into π-loaded chalcogenido–imido and bis(chalcogenido) complexes. We end by summarizing trends in reactivity and provide predictions of promising classes of complexes for future researchers to target. This Perspective only covers the chemistry of π-loaded group 5 bis(imido) and chalcogenido–imido complexes; the extensive chemistry of group 3–6 mono- and bis(imido) complexes has been reviewed elsewhere.[1–4,12,35–37]

2. Structure of π-loaded bis(imido) complexes

A commonly employed approach to π-loading in group 5 transition metal complexes involves incorporation of the bent bis(imido) motif. Putative π-loaded tris(imido) complexes of Nb(v) and Ta(v) have also been reported, but crystallographic characterization of these complexes was tenuous, and their

Sacy Lopez-Flores is an undergraduate student in the College of Letters & Science at the University of California, Berkeley, and is majoring in Molecular and Cell Biology. She is currently studying the transition metals in the 5th group of the periodic table. She is interested in genetics and DNA in the human body system.

Robert G. Bergman is Professor Emeritus and Professor of the Graduate School, recalled for research and part-time teaching in the College of Chemistry at the University of California, Berkeley. His current research is collaborative, focusing on synthetic and mechanistic studies of stoichiometric and catalytic reactions involving early metal complexes and supramolecular systems.

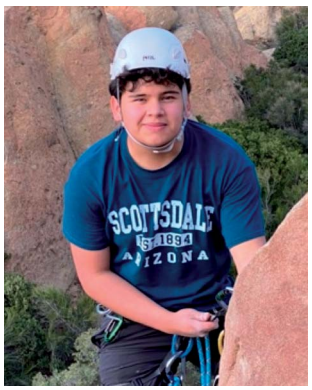

Diego Alcantar is an undergraduate in the College of Chemistry at the University of California, Berkeley. He is currently studying group 5 transition metals. He has an interest in electrochemistry, particularly in the development of electrochemical cells.

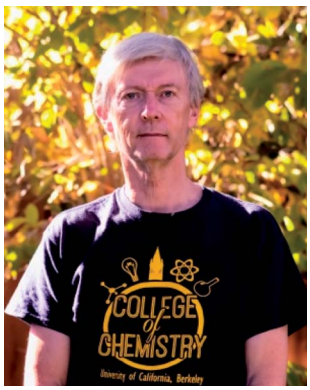

John Arnold is a Professor of Chemistry and Undergraduate Dean in the College of Chemistry at UC Berkeley. He is a graduate of the University of Salford (Applied Chemistry, 1982) and the University of California, San Diego (PhD with Prof. T. D. Tilley, 1986). He carried out postdoctoral work with Professor Sir Geoffrey Wilkinson at Imperial College, London from 1987 to 1988 before a short stint as a Royal Society University Research Fellow (1988 to 1989). He began his independent career at UC Berkeley as an assistant professor in 1989.

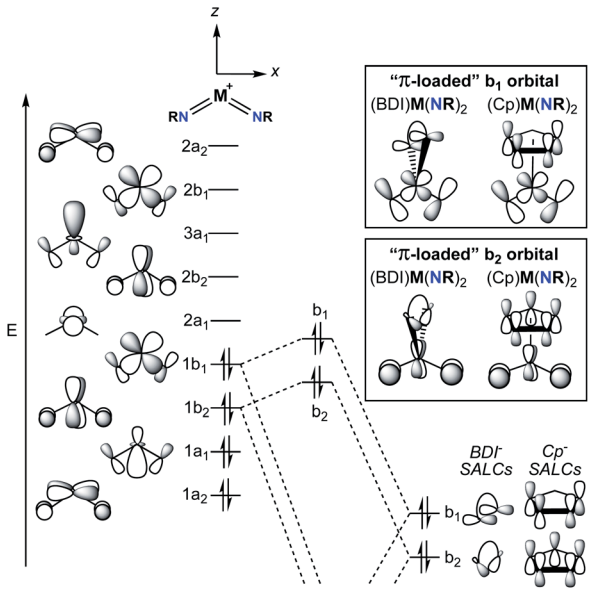

Fig. 2 Molecular orbitals for the $[M(NR)_2]^+$ fragment (left, M = V, Nb, Ta), selected symmetry adapted linear combinations (SALCs) of molecular orbitals for a cyclopentadienyl (Cp) ancillary ligand and a β-diketiminate (BDI) ancillary ligand (right), and relative energy and symmetry considerations for the combination of the $[M(NR)_2]^+$ fragment and a monoanionic, π-donor ligand (center). Relative energies of molecular orbitals are not drawn to scale.

reactivity remains to be studied.[31] The π-loading strategy is summarized in the qualitative molecular orbital diagram depicted in Fig. 2.[29,38,39] On the left side of the diagram, the molecular orbitals (MOs) for the C_{2v}-symmetric $[M(NR)_2]^+$ (M = V, Nb, Ta) fragment are shown. The relative ordering of the MOs depends on the angle between the two imido groups; for angles larger than *ca.* 130°, the energy of the $1b_1$ MO drops below that of the $1b_2$ MO.[38] In other words, depending on the angle between the imido groups, the HOMO is either the $1b_1$ or $1b_2$ MO. That being said, N_{imido}–M–N_{imido} (M = V, Nb, Ta) bond angles that lie below the ideal angle of 120° are most common, often approaching 90°, as this geometry permits better orbital overlap between imido-based σ- and π-donor orbitals with metal atomic orbitals.[39] In either case, the HOMO ($1b_1$ or $1b_2$) consists of metal–imido bonding orbitals; this is consistent with the observation that bis(imido) complexes tend to react at one of the two metal-imido groups. Calculations have suggested that the nonbonding LUMO ($2a_1$) is composed of a linear combination of metal d_{z^2} and $d_{x^2-y^2}$ orbitals, with large lobes oriented along the *y*-axis (effectively a d_{y^2} orbital).[38]

The nonbonding LUMO ($2a_1$), antibonding LUMO+1 ($2b_2$), and antibonding LUMO+2 ($3a_1$) are oriented along a plane bisecting the two imido ligands (the *yz* plane). These unoccupied orbitals lack any π-bonding component in the *xz* plane. As such, incorporation of a π-donor ligand at these positions would cause competition between the π-donor ligand and the occupied metal-based π-symmetry MOs ($1b_1$ and $1b_2$), causing the energy of the HOMO and HOMO-1 ($1b_1$ and $1b_2$) to increase.[29] On the right side of Fig. 2, this phenomenon is depicted for two commonly employed monoanionic π-donor ligands in the early transition metal literature: cyclopentadienyl and β-diketiminate.

Computational investigations into three different group 5 bis(imido) systems provide support for the qualitative molecular orbital diagram shown in Fig. 2. First, the C_{2v}-symmetric, cationic vanadium bis(imido) complexes $[V(PEt_3)_2(N^tBu)_2]^+$ and $[V(\eta^1\text{-CO})(PEt_3)_2(N^tBu)_2]^+$ were optimized at the B3LYP level of density functional theory (DFT), with the goal of gaining insight into the nature of V → CO π-back bonding in this system.[40] The N_{imido}–V–N_{imido} bond angle in the optimized CO-adducted complex was found to be 118.4°. In line with this small N_{imido}–V–N_{imido} angle, the HOMO is suggested to be b_1-symmetric for both complexes, while the HOMO-1 is b_2-symmetric. Calculations suggest the π* orbitals of CO interact with the b_1-symmetric HOMO of the base-free complex $[V(PEt_3)_2(N^tBu)_2]^+$, generating a lower-energy bonding combination (the HOMO of $[V(\eta^1\text{-CO})(PEt_3)_2(N^tBu)_2]^+$) and a higher-energy antibonding combination. The b_2-symmetric orbitals of $[V(PEt_3)_2(N^tBu)_2]^+$ are also involved in π-back bonding to CO in this system. Thus, π-back bonding interactions in this system serve to lower the energy of the imido-based HOMO and HOMO-1, decreasing the effects of π-loading.

Second, the complex (BDI′)Nb(NMe)$_2$ (BDI′ = HC[C(Me)N(2,6-Me_2-C_6H_3)]$_2$) was optimized at the BP86 level of DFT.[29] The optimized structure was C_{2v} symmetric, with a N_{imido}–Nb–N_{imido} bond angle of 110.8°. The HOMO-1 was suggested to be b_2-symmetric and polarized toward the imido nitrogen atoms (11.5% metal character, 53.3% imido nitrogen p-character, 6.8% BDI-ligand p-character). The HOMO of the optimized complex was suggested to be the antibonding combination of the b_1-symmetric $[Nb(NMe)_2]^+$ fragment and the BDI ligand (5.5% metal character, 47.4% imido nitrogen p-character, 33.1% BDI-ligand p-character). The lower energy bonding combination of the b_1-symmetric orbitals was suggested to be primarily composed of BDI-ligand p-character (9.5% metal character, 19.6% imido nitrogen p-character, 52.2% BDI-ligand p-character). The composition of these orbitals and their energies relative to related orbitals in the $[Nb(NMe)_2]^+$ fragment suggest that π-loading does indeed increase the energy and polarization of the imido-based HOMO and HOMO−1 in this system.

Third, a computational study was carried out to investigate the bonding in the dimeric bis(imido) complex [(CCC)Ta(N^tBu_2)·LiI]$_2$ (CCC = 2,6-(^{Bu}Im)$_2$-C_6H_3, Im = imidazole) at the PBEPBE level of DFT.[32] The HOMO and HOMO−1 of the optimized complex were suggested to both be π-symmetric imido N-centered (*ca.* 45%) orbitals; the N_{imido}–Ta–N_{imido} bond angle in the optimized complex was not given. Thus, in all three cases presented above, the HOMO is localized on the bis(imido) groups, consistent with imido-based reactivity patterns displayed by these types of complexes.

In addition to computational studies, the electronic structure of vanadium bis(imido) complexes has been investigated *via* X-ray absorption near-edge structure (XANES) spectroscopy and ^{13}C and ^{51}V nuclear magnetic resonance (NMR) spectroscopy. A systematic study of complexes V(N^tBu)$_2$ClL$_2$ (L = PMe_3, PEt_3, PMe_2Ph) and V(N^tBu)$_2$(PMe_3)$_2$X (X = Cl, I, Br) by La Pierre

et al. revealed the electronic structure in these complexes to be dominated by the imido ligands.[41] For the family of complexes that varies by identity of the phosphine donor ligand, all three spectroscopic studies suggested that donating ability and steric profile of the variable ligand influences electronic structure: larger cone angles and more electron-rich phosphines led to increased localization of electron density at the imido groups. However, the overall trends in the spectroscopic data of this family of complexes were quite subtle. Furthermore, for the halide family, no discernable trends in the data could be observed. These data stand in contrast to reported ^{51}V NMR trends displayed by the well-studied family of complexes $CpV(NR)X_2$ (X = Me, Cl, Br, I), where the identity of the X ligand has dramatic consequences on the electronic structure of the complex.[42–45] Thus, the data reported by La Pierre *et al.* suggest that the electronic structure in these complexes is dominated by π-bonding interactions with the imido ligands, with little influence from the other ligands present.

Finally, the effects of π-loading manifest in increased bond lengths for M-imido groups in bis(imido) complexes, relative to their mono(imido) congeners. In Fig. 3, we present eight pairs of closely related group 5 bis(imido) and mono(imido) complexes,

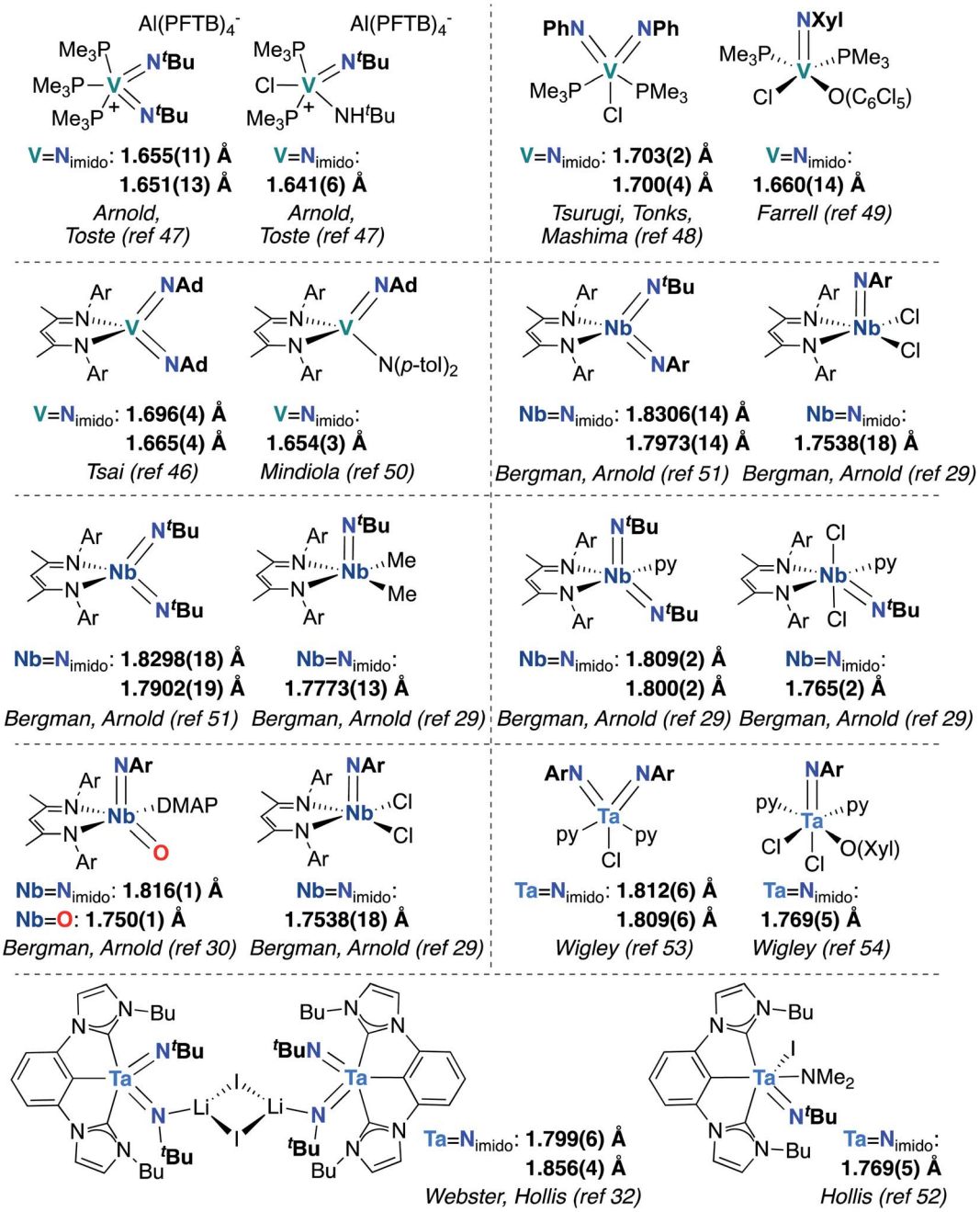

Fig. 3 Crystallographically characterized pairs of closely related group 5 bis(imido) (or oxo-imido) and mono(imido) complexes, with M=N_{imido} (or M=O) bond lengths in Å. Ar = 2,6-diisopropylphenyl.

as well as an oxo-imido complex and a closely related mono(imido) complex. Pairs of complexes were selected such that the oxidation state at the metal center and net charge on the complex are identical in all cases, while the identity of supporting ligand(s) and imido substituent group(s) are as similar as possible. In all cases, the crystallographically determined M=N bond lengths displayed by π-loaded bis(imido) or oxo-imido complexes are lengthened relative to their mono(imido) congeners, suggesting that π-loading serves to weaken the M-imido interaction and therefore increase reactivity of M-imido groups in these complexes. Indeed, in all but one of the cases presented below, the bis(imido) complex reacts across one of the two imido groups either *via* 1,2-addition or cycloaddition (no reactivity was reported for Tsai and coworker's (BDI)V(NAd)$_2$ complex[46]). Of particular note is the Nb oxo-imido complex (BDI)NbO(NAr)DMAP, which reacts *via* 1,2-addition across the π-loaded oxo group.[30] In contrast, none of the mono(imido) complexes presented in Fig. 3 display imido-based reactivity.[29,47,49,50,52,54] These opposing reactivity trends serve to drive home our point: the imido moieties in group 5 mono(imido) complexes tend to serve solely as supporting ligands, whereas π-loaded group 5 bis(imido) complexes display reactive imido groups. These reactivity patterns are detailed in the following section.

3. Synthetic routes to group 5 bis(imido) complexes

Bis(imido) complexes are typically accessed from mono(imido) precursors *via* one of several routes, as outlined in Fig. 4: (1) oxidation of a d^2 imido precursor;[46,48,55–58] (2) base-induced α-elimination from an imido-amido precursor;[39,41,59] and (3) α-hydrogen elimination from an imido-amino-halide precursor.[29,32,53,60] The first route necessitates generating a low-valent imido precursor; d^2 group 5 transition metals are known to be highly reactive, so if the precursor is to be isolated, bulky supporting ligands are required to enforce kinetic stability.[61] Masking of low valence *via* π-back bonding with arene or CO ligands can also help in isolating stable low valent precursors: for example, Bergman and Arnold have demonstrated facile Nb bis(imido) synthesis *via* reaction of the Nb(III) complex (BDI)Nb(N^{t}Bu)(η^6-C$_6$H$_6$) with various organic azides.[57] In other cases, a low valent intermediate can be generated *in situ*: Tsurugi, Tonks, and Mashima were able to generate V(NPh)$_2$Cl(PMe$_3$)$_2$ upon reduction of V(NPh)Cl$_3$ in the presence of azobenzene, followed by addition of PMe$_3$.[48]

The second route depicted in Fig. 4 is commonly employed to access sterically unencumbered bis(imido) complexes supported by labile ligands. For example, Wolczanski found that heating the mono(imido) complex Ta(NHSi^{t}Bu$_3$)(NSi^{t}Bu$_3$)Me$_2$ in pyridine or THF led to generation of the bis(imido) complex Ta(NSi^{t}Bu$_3$)$_2$MeL$_2$ (L = py, THF) and methane.[39] Elimination of silyl chlorides can also provide impetus for formation of bis(imido) complexes: La Pierre *et al.* reported an imido-silylamido precursor V(N^{t}Bu)(N(TMS)^{t}Bu)Cl$_2$ that liberated TMSCl upon addition of a Lewis base and heat to yield complexes V(N^{t}Bu)$_2$ClL$_2$ (L = PMe$_3$, PEt$_3$, PMe$_2$Ph, py).[41]

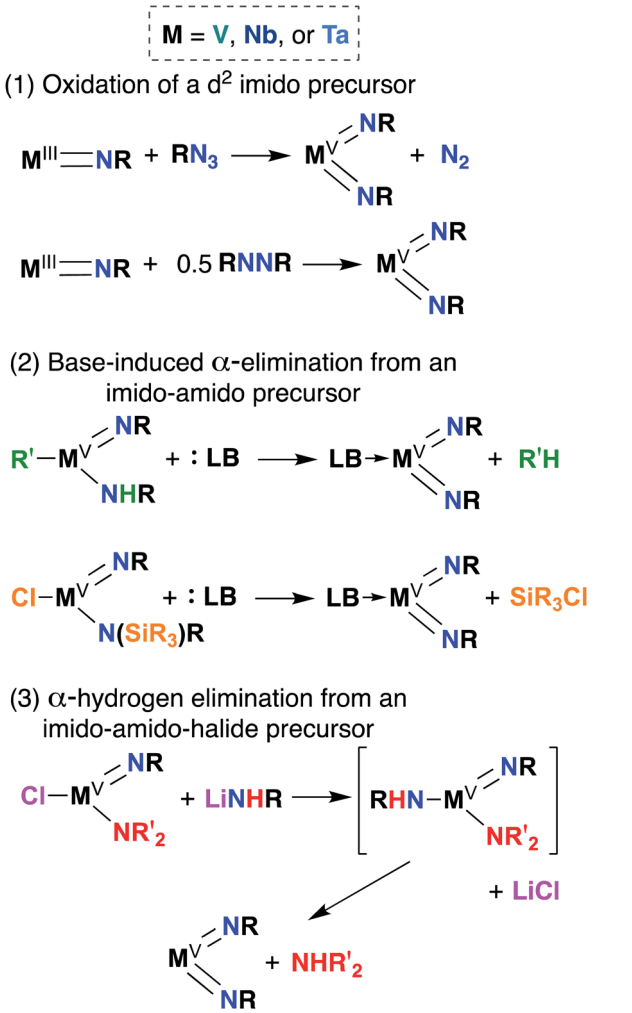

Fig. 4 Synthetic routes to group 5 bis(imido) complexes.

Finally, the third route shown in Fig. 4 stands alone in that it can be employed to synthesize bis(imido) complexes directly from amido-halide precursors in a one-pot, multistep synthesis (although this route is also commonly employed starting from imido-amido-halide precursors, as depicted). This route was pioneered by Wigley, who reported synthesis of M(NDipp)Cl(py)$_2$ (M = Nb, Ta) *via* reaction of two equivalents of LiNH(Dipp) with either Ta(NEt$_2$)$_2$Cl$_3$(OEt$_2$) or [Nb(NEt$_2$)$_2$Cl$_3$]$_2$.[53] In the same work, Wigley showed that the Ta bis(imido) product could be also isolated upon reaction of Ta(NDipp)(NEt)$_2$Cl$_2$(py)$_2$ with one equivalent of LiNH(Dipp). As with route 2, route 3 can provide access to sterically unencumbered bis(imido) complexes supported by labile ligands.

4. Reactivity of π-loaded bis(imido) complexes

4.1. Catalytic reactions mediated by group 5 bis(imido) complexes

To date, there have been four reports of catalytic transformations mediated by group 5 metal bis(imido) complexes; all

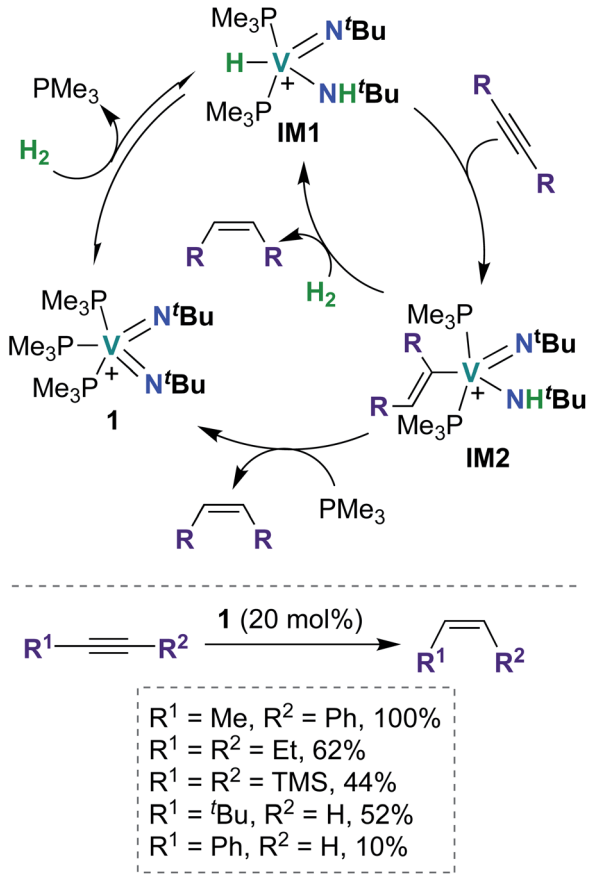

Scheme 1 V bis(imido)-catalyzed semihydrogenation of alkynes to *Z*-alkenes.

reports suggest key elementary steps that occur across a metal–imido bond. In 2011, La Pierre *et al.* reported cationic V(v) bis(imido) **1** (Scheme 1), supported by labile trimethyl phosphine ligands, that was capable of mediating *Z*-selective semihydrogenation of alkynes.[47] V bis(imido) complexes are relatively rare, and there are only a handful of other cationic V bis(imido) complex reported to date.[40,41] When a solution of **1** was placed under an atmosphere of H_2, the authors observed spectroscopic evidence of equilibrium between **1** and hydrido-imido-amido intermediate **IM1** (Scheme 1), the product of 1,2-addition of H_2 across the V–imido bond. In the presence of alkynes and H_2, **1** readily and selectively converted alkynes to *Z*-alkenes, with 44–100% conversion rates observed for internal aryl, alkyl, and silyl alkynes. Significantly lower yields (10–52%) were observed with terminal aryl and alkyl alkynes, presumably due to competitive addition of the terminal C–H bond across the π-loaded V-imido group.

Using a combination of synthetic and computational studies, the authors proposed two likely catalytic mechanisms, as outlined in Scheme 1. First, H_2 undergoes 1,2-addition across one of the V–imido bonds to generate **IM1**. One equivalent of alkyne then inserts into the V–hydrido bond to yield imido-amido-alkenyl **IM2**. Intermediate **IM2** can then undergo σ-bond metathesis with another equivalent of H_2 to give **IM1** (center route) or undergo 1,2-α-NH elimination to yield **1** (left route). A combination of H_2/D_2 crossover experiments and parahydrogen-induced polarization NMR experiments provided strong support for the path involving 1,2-α-NH elimination (left route): both sets of experiments suggested that a single molecule of H_2 is involved in reduction of the alkyne substrate. Three features of catalyst **1** likely contribute to its unique catalytic ability: π-loaded imido groups, positive charge (the neutral analogue to **1** was not found to be catalytically active), and labile supporting ligands.

In 2019, Tonks, Mashima, and co-workers found that a combination of $VCl_3(THF)_3$ and *N*,*N*-bis(trimethylsilyl)aniline is an efficient catalyst for the [2 + 2 + 1] coupling reaction of alkynes and azobenzenes to yield substituted pyrroles; they obtained strong evidence supporting V bis(imido) intermediate **IM4** (Scheme 2) as the catalytically active species.[48] Preliminary catalyst screening experiments indicated that formation of bis(imido) V species is important to catalysis: under catalytic conditions, a combination of mono(imido) complex $VCl_3(NPh)$ and *N*,*N*-bis(trimethylsilyl)aniline produced the desired pyrrole product in quantitative yield, while in the absence of azobenzene, $VCl_3(NPh)$ resulted in poor yield (6%) of the desired product. Substrate scope was investigated, as detailed in the bottom of Scheme 2: highest yields were obtained upon combining azobenzene with symmetrical aliphatic alkenes, such as 3-hexyne (74%) and 4-octyne (92%).

Kinetic studies revealed a second-order rate dependence on $VCl_3(THF)_3$, suggesting bimetallic activation of azobenzene by a V species; it was found to be first-order with respect to 5-decyne and 0.8-order with respect to azobenzene. The authors suggested that a V(III) mono(imido) species was responsible for azobenzene cleavage, yielding a V(v) bis(imido) species. To test this hypothesis, $V(NPh)Cl_3$ was treated with an organosilicon reducing reagent[62] in the presence of azobenzene and 5-decyne to yield "V(NPh)Cl", as evidenced by observation of two equivalents of $SiMe_3Cl$ by ^1H NMR spectroscopy. Upon heating this reaction mixture, 91% conversion to the desired pyrrole product was observed, indicating that similar mono(imido) V(III) and bis(imido) V(v) species may be generated along the catalytic cycle. Additionally, the authors were able to trap a V(v) bis(imido) species by generating V(NPh)Cl *in situ* as described above, followed by subsequent addition of PMe_3 to yield bis(imido) V(v) **2** (Scheme 2). Complex **2** was subsequently demonstrated to be a competent catalyst for the [2 + 2 + 1] coupling reaction; this experiment clearly indicates that a V(v) bis(imido) species is catalytically relevant.

Based on these kinetic and other experimental studies, the authors proposed a mechanism for the coupling of azobenzene and 5-decyne, as outlined in Scheme 2: first, reaction of $VCl_3(THF)_3$ with *N*,*N*-bis(trimethylsilyl)aniline yields the on-cycle mono(imido) V(III) species **IM3**, with concomitant generation of two equivalents of $SiMe_3Cl$. Then, bimetallic reductive cleavage of azobenzene furnishes bis(imido) V(v) intermediate **IM4**, which subsequently reacts with alkyne *via* [2 + 2] cycloaddition to form azavanadacyclobutene **IM5**. Next, a second equivalent of alkyne inserts into the V–C bond to form azavanadacyclohexadiene **IM6**; reductive elimination from **IM6** yields the substituted pyrrole product and a mono(imido) V(III)

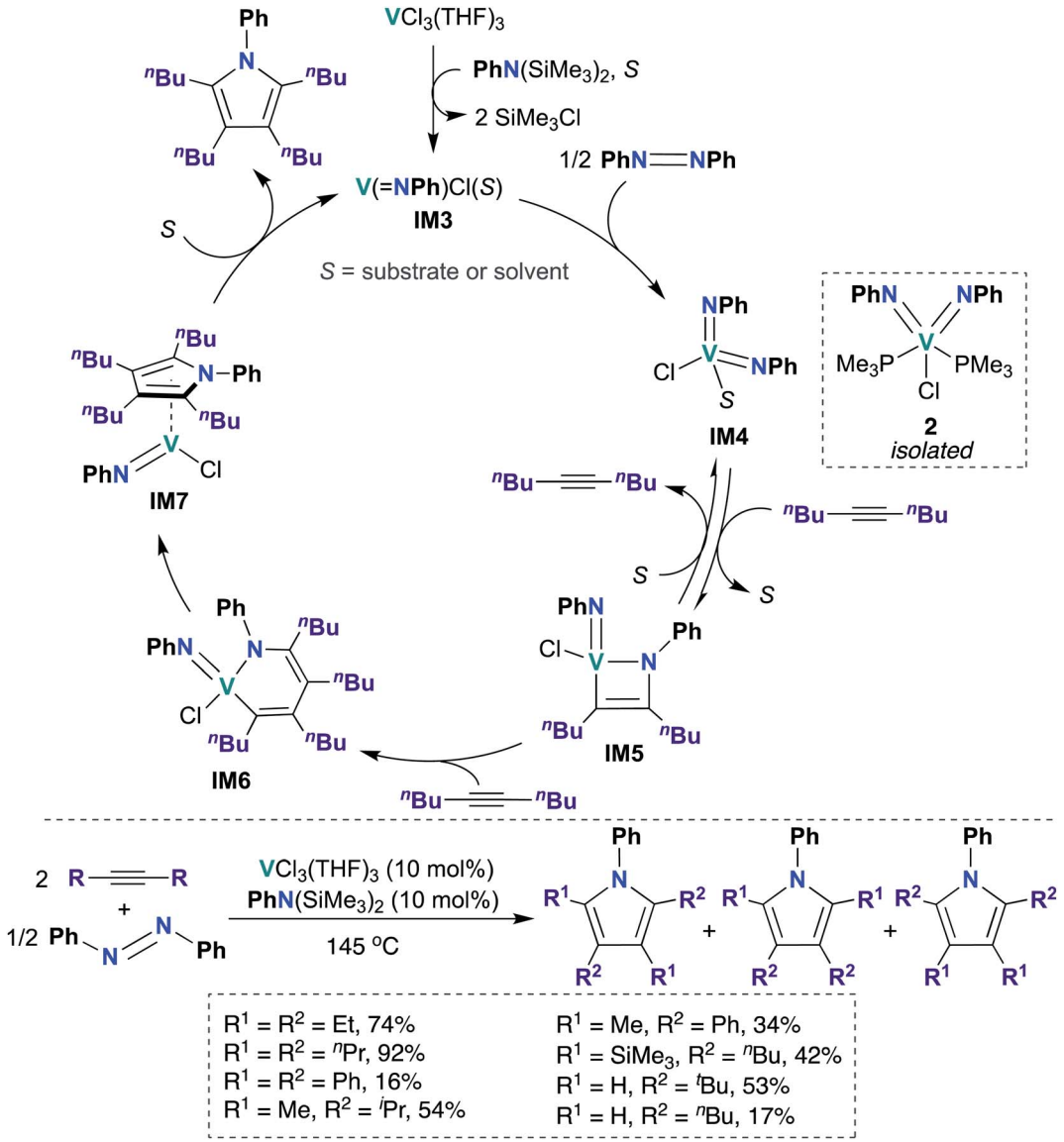

Scheme 2 V bis(imido)-catalyzed [2 + 2 + 1] coupling of alkynes and azobenzenes to give multisubstituted pyrroles.

intermediate **IM7**, which may be stabilized by back-bonding to pyrrole product. Finally, dissociation of pyrrole regenerates mono(imido) V(III) species **IM3**, thus completing the catalytic cycle.

A 2015 report by Bergman, Arnold, and co-workers detailed a series of BDI-supported Nb bis(imido) complexes capable of mediating stoichiometric nitrene transfer reactions, as well as catalytic nitrene transfer from organic azides and isocyanides to yield asymmetric dialkylcarbodiimines.[57] Four-coordinate bis(imido) Nb complex **3** (Scheme 3, top) reacts with isocyanide to give five-coordinate bis(imido) **4-Xyl**. When this complex was subjected to heat, either in solution or in the solid state, clean conversion to five-coordinate bis(imido) **5-Xyl** was observed, in which the nitrene fragments from one *tert*-butyl imido group and the coordinated isocyanide were exchanged to generate a complex containing a thermodynamically favored aryl(imido) ligand and coordinated *tert*-butyl isocyanide. Complexes **5-R** (R = 2,6-dimethylphenyl, 4-methoxy-2,6-dimethylphenyl, or 4-methoxyphenyl) could also be generated from **3** upon heating in the presence of the appropriate aryl isocyanide. The authors hypothesized that these stoichiometric transformations occurred *via* an η^2-carbodiimide mono(imido) intermediate, akin to **IM8** in the bottom of Scheme 3. This work represents the only example of exchange of nitrene groups to generate a new isocyanide and imido group, which could potentially be leveraged as a new method for incorporation of imido moieties into metal complexes and integration of various substituents into isocyanides.

Inspired by these results, the authors considered whether these complexes could carry out catalytic nitrene transfer. They found that addition of excess *tert*-butyl azide and alkyl isocyanide to **4-Ak** (Scheme 3, bottom; Ak = *n*-butyl, cyclohexyl, or benzyl) resulted in catalytic generation of asymmetric carbodiimides upon heating, as observed by ^{1}H NMR spectroscopy.

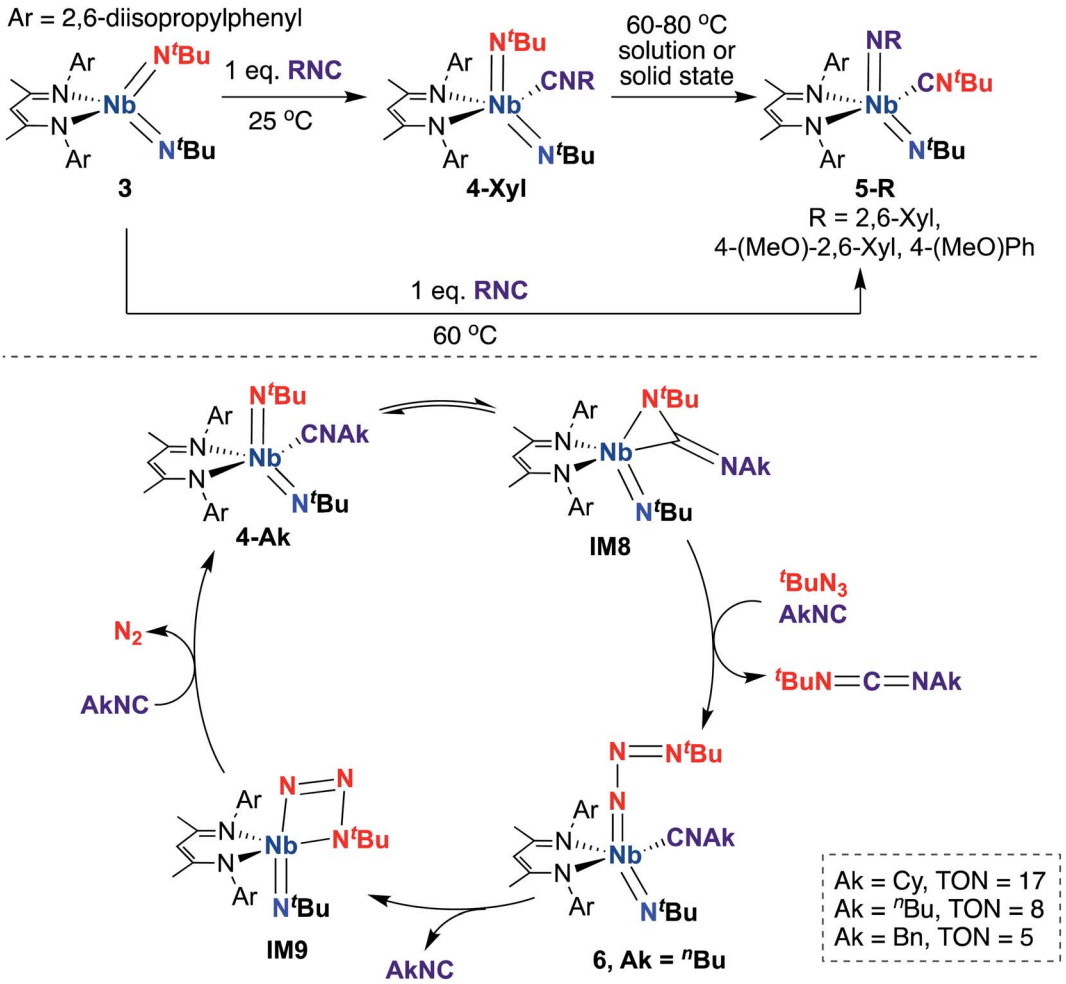

Scheme 3 Nb bis(imido)-promoted stoichiometric nitrene metathesis (top) and catalytic nitrene transfer from organic azides and isocyanides to give dialkylcarbodiimides (bottom).

Notably, they observed build-up of an intermediate by ^{1}H NMR spectroscopy under catalytic conditions. Upon leaving a mixture of **4-^{n}Bu**, excess *tert*-butyl azide, and *n*-butyl isocyanide undisturbed at room temperature for several hours, single crystals of terminal *tert*-butylazido mono(imido) **6** (Scheme 3, bottom) were obtained; isolated **6** was found to be a competent catalyst for carbodiimide formation. Based on these experimental results, the authors proposed the mechanism outlined in the bottom of Scheme 3. Upon heating, **4-Ak** reaches dynamic equilibrium with η^2-carbodiimide mono(imido) intermediate **IM8**, in which coordinated isocyanide has inserted into one of the two Nb-imido groups. Then, **IM8** eliminates asymmetric alkylcarbodiimide, coordinates isocyanide, and reductively binds organic azide to generate terminal azido **6**. Next, coordinated isocyanide is released to open a binding site at the metal center, allowing generation of azaniobacycle intermediate **IM9**, which subsequently liberates N_2 and binds isocyanide to regenerate **4-Ak** and complete the catalytic cycle.

In 2016, Hollis, Webster, and co-workers reported Ta bis(imido) **7** (Scheme 4), supported by a tridentate, monoanionic pincer ligand with two *N*-heterocyclic carbene donor groups, that is capable of catalytically mediating intermolecular transfer hydrogenation of α,ω-aminoalkenes to yield cyclic imines, cyclic amines, and hydrogenated substrate.[32] Upon heating **7** in the presence of various α,ω-aminoalkenes (Scheme 4, bottom), complete conversion to a distribution of three products was observed: a cyclic imine, the product of oxidative amination; a monosubstituted amine, the product of reductive hydrogenation; and a smaller amount of a cyclic amine, the product of intramolecular hydroamination.

Varying reaction conditions led to different product distributions, with shorter reaction times favoring the oxidative amination product. In line with this experimental observation, a computational study suggested that the oxidative amination product is favored kinetically, while hydrogenated substrate is the thermodynamic product.[63] Secondary amines did not react under catalytic conditions, suggesting that **7** initially reacts with the substrate *via* imido ligand exchange to form a Ta-imidoalkene species. Based on these experimental and computational investigations, the authors propose a possible, albeit complex, mechanistic pathway. A key elementary step in the transformation involves intramolecular [2 + 2] cycloaddition across Ta-imido groups to give an azatantallacyclobutane intermediate.

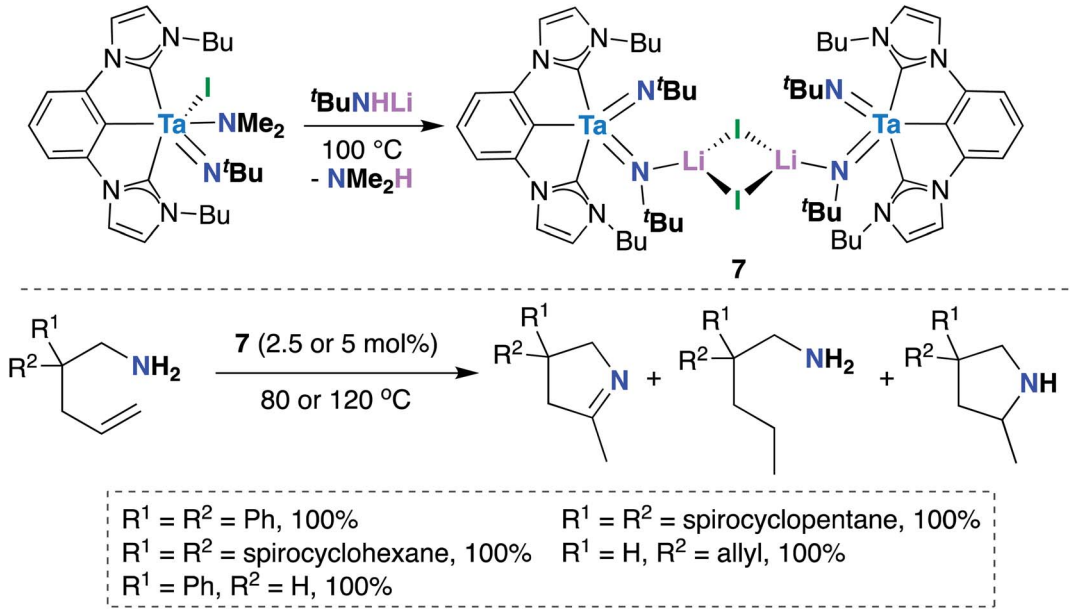

Scheme 4 Ta bis(imido)-catalyzed oxidative amination of alkenes to yield cyclic imines, cyclic amines, and hydrogenated substrate.

4.2. Stoichiometric reactivity of group 5 bis(imido) complexes

While reports of group 5 bis(imido)-catalyzed processes are relatively rare and have only been reported within the last decade, examples of stoichiometric reactivity across a π-loaded group 5 metal–imido bond are more numerous, particularly for Nb, with reports dating back to the early 1990s. Reactivity patterns include 1,2-additions, reductive eliminations, and overall [2 + 2], [2 + 4], and [3 + 2] cycloadditions and retro-cycloadditions. Below, we outline these examples of stoichiometric reactivity, starting with V and moving to Nb and then to Ta.

4.2.1. Stoichiometric reactivity of vanadium bis(imido) complexes. In 1993, de With and Horton reported the mono-(imido) complex V(NSi^{t}Bu$_3$) (NHSi^{t}Bu$_3$)$_2$Me **8** (Scheme 5) and

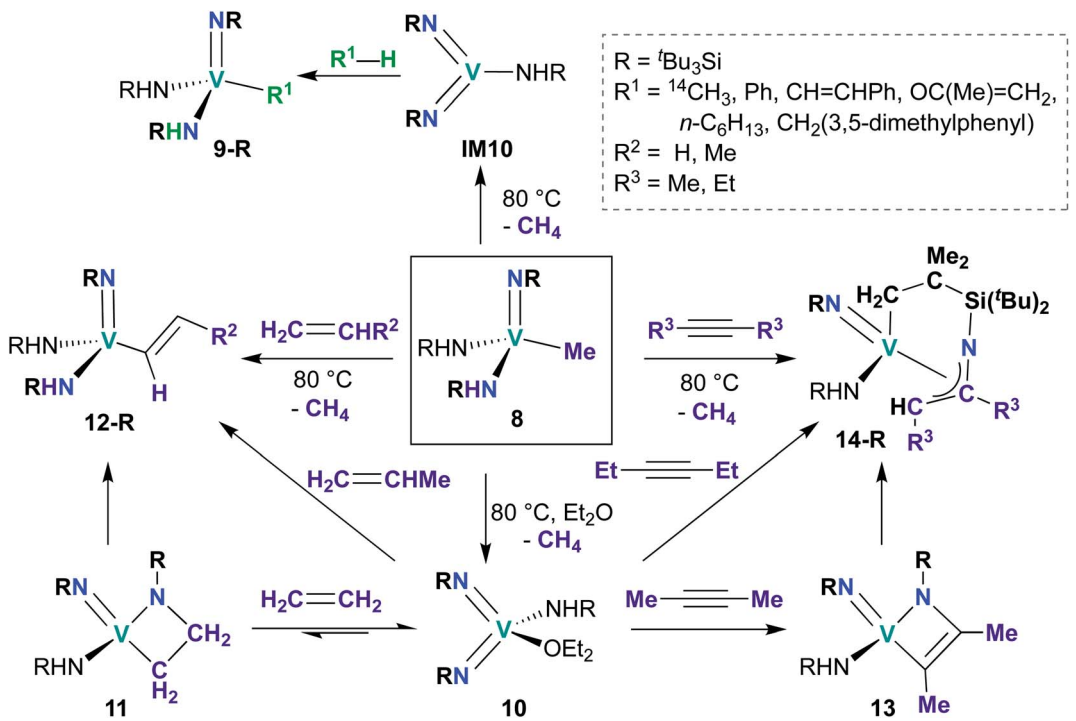

Scheme 5 1,2-Addition and [2 + 2] cycloaddition reactivity of V bis(imido) complexes.

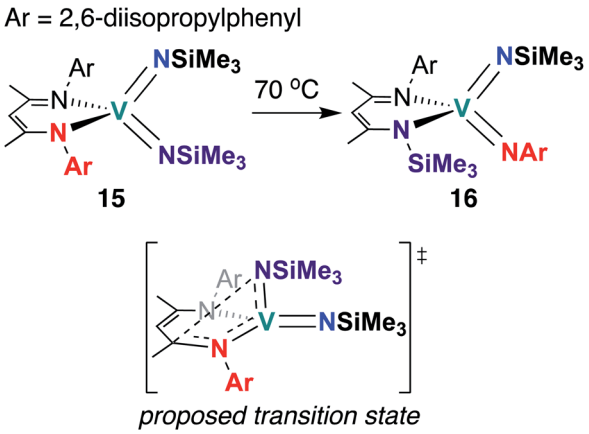

Scheme 6 Intramolecular ligand insertion reactivity of a V bis(imido) complex.

detailed its 1,2-addition reactivity with various alkanes, alkynes, benzene, and acetone to yield products **9-R** (R = Me, Ph, CH = CHPh, OC(Me) = CH_2, *n*-C_6H_{13}, CH_2(3,5-dimethylphenyl).[64] The authors posited that these reactions occurred *via* liberation of methane to generate the transient bis(imido) intermediate **IM10**, which then activated substrates *via* 1,2-addition across one of the V–imido bonds. Support for this proposal is twofold: first, reaction of **8** with benzene-d_6 yielded CH_4 as a side product, indicating that C–D activation of benzene-d_6 does not occur *via* a simple σ-bond metathesis mechanism, and second, bis(imido) **10** could be isolated upon heating **8** in the presence of Et_2O.

A subsequent report detailed [2 + 2] cycloadditions of imido-amido **8** and bis(imido) **10** (Scheme 5).[59] Mono(imido) **8** reacts with alkenes to yield alkenyl complexes **12-R** (R = H, Me), and with alkynes to yield η^3-azallyl complexes **14-R** (R = Me, Et). These reactions presumably proceed through bis(imido) intermediate **IM10**, which subsequently undergoes [2 + 2] cycloaddition of alkene or alkyne across an Nb-imido bond, followed by isomerization to yield the final product. Products **12-R** and **14-R** could also be synthesized *via* addition of alkene or alkyne to base-stabilized bis(imido) **10**; vanadaazacyclobutane **11** and vanadaazacyclobutene **13** could be isolated from these reactions.

The third and final example of stoichiometric V bis(imido) reactivity was published in 2010 by Tsai and co-workers, who synthesized a series of V bis(imido) complexes, (BDI)V$(NR)_2$ (R = *p*-tolyl, 1-adamantyl, $SiMe_3$) and observed that trimethylsilyl analogue **15** (Scheme 6) underwent isomerization to the mixed 2,6-diisopropylphenylimido-trimethylsilylimido **16** upon heating.[46] Kinetic studies suggested that this transformation proceeds intramolecularly *via* the proposed transition state depicted in Scheme 6.

4.2.2. Stoichiometric reactivity of niobium bis(imido) complexes. Reactive Nb bis(imido) systems have thus far only been reported by Arnold, Bergman, and co-workers, over the last decade. In all cases, the Nb bis(imido) fragment is supported by a bulky, bidentate, monoanionic ligand, either BDI or mono-azabutadiene (MAD), which is formed upon reductive cleavage of the BDI ligand. The structures of all numbered complexes in Schemes 7–14 were established using X-ray diffraction studies,

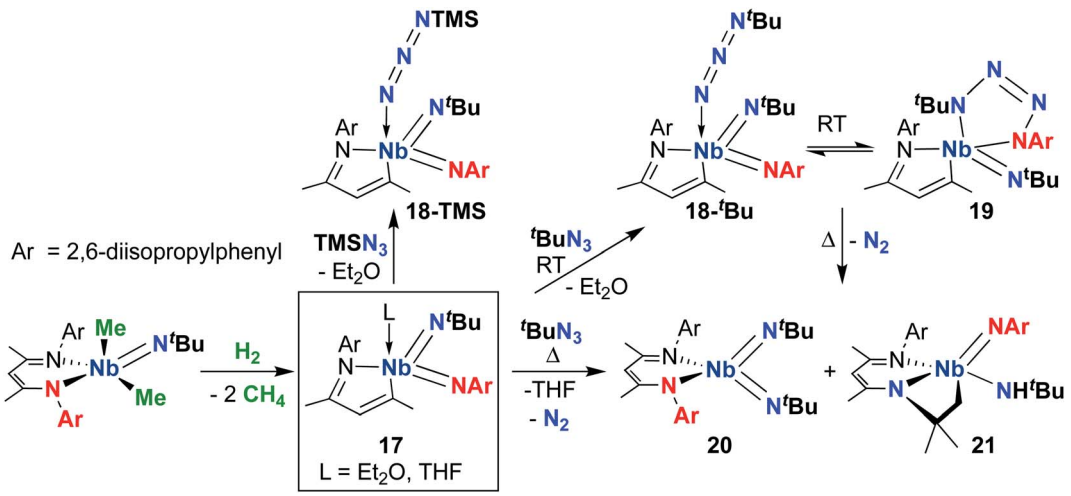

Scheme 7 Reactivity of a MAD-supported Nb bis(imido) complex with organic azides.

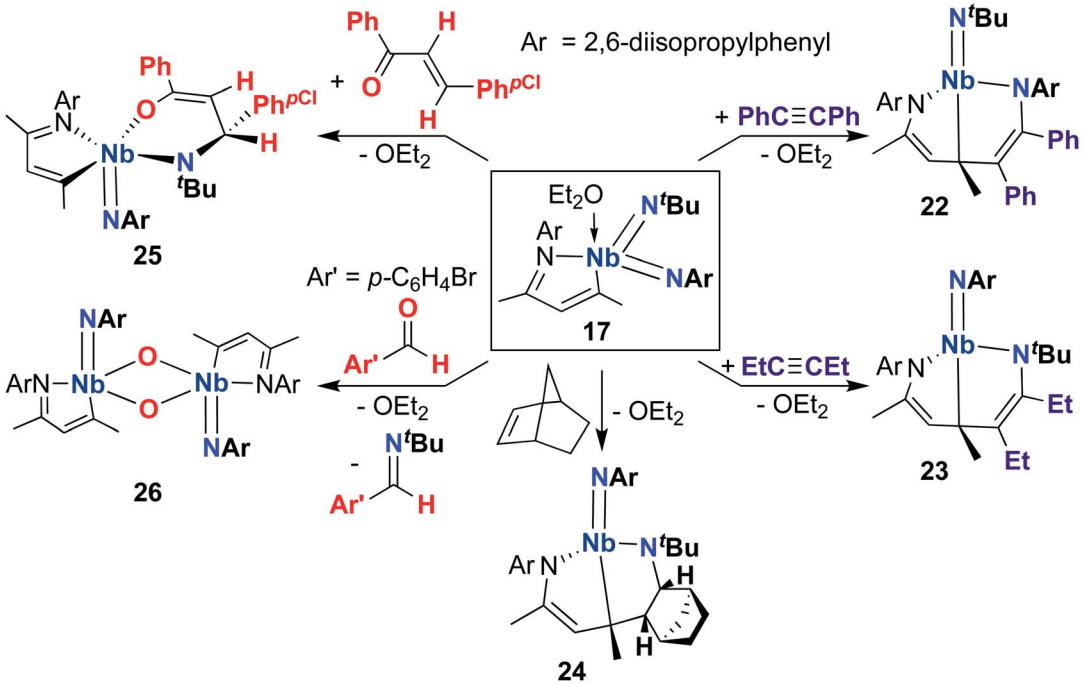

Scheme 8 [4 + 2] and [2 + 2] cycloaddition reactivity of a MAD-supported Nb bis(imido) complex.

while spectroscopically observed species are given IM labels (denoting these species as intermediates).

Focusing on the MAD system first, a 2014 report detailed synthesis of MAD-supported Nb bis(imido) **17** (Scheme 7) from reaction of a BDI-supported mono(imido) dimethyl complex with H_2.[51] The presumed low-valent intermediate, (BDI)Nb(N^{t}Bu), is unstable and reductively cleaves the BDI ligand to form a high-valent bis(imido) complex. Intriguingly, **17** reacted with organic azides to give bis(imido) complexes **18-R** (R = trimethylsilyl, *tert*-butyl), which featured a rare example of a terminally-bound, unreduced azide ligand. A variable temperature NMR study revealed that *tert*-butyl derivative **18-tBu** exists in dynamic equilibrium with niobatetrazene **19**, the product of [3 + 2] cycloaddition of an organic azide across a π-loaded Nb-imido group; such cycloadditions are rare in the early transition metal literature.[65–67] Remarkably, heating this equilibrating mixture to temperatures above 35 °C resulted in unprecedented reformation of the BDI ligand, yielding complexes **20** and **21** in an 85 : 15 ratio. Complex **21** presumably arose from a four-coordinate bis(imido) complex, which undergoes C–H activation across the Nb-(*tert*-butyl)imido group. The remarkable reactivity of bis(imido) **20** is reported in subsequent publications (see below).

A 2015 publication detailed cycloaddition reactivity of MAD-supported bis(imido) **17** with unsaturated substrates (Scheme 8).[68] Addition of acetylene or hex-3-yne to **17** resulted in formation of complexes **22** and **23**, each bearing an eight-membered metallacycle composed of the MAD ligand, an imido group, and a substrate C–C multiple bond. DFT calculations suggested this transformation involves initial [2 + 2] cycloaddition of alkyne across one of the Nb-imido moieties to yield an azaniobacyclobutene intermediate, followed by conjugative addition of the newly formed Nb–C bond to the MAD ligand. The authors suggested that the observed regioselectivity (*i.e.*, reactivity occurs at either the (*tert*-butyl)imido or (2,6-diisopropylphenyl)imido group) arises due to different activation energies for the conjugative addition step. Similarly,

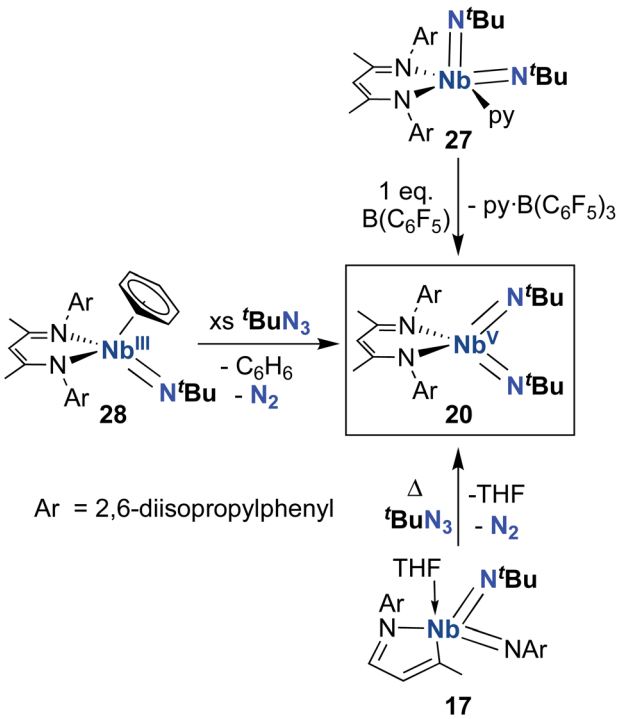

Scheme 9 Synthetic routes to the symmetric Nb bis(imido) complex **20**.

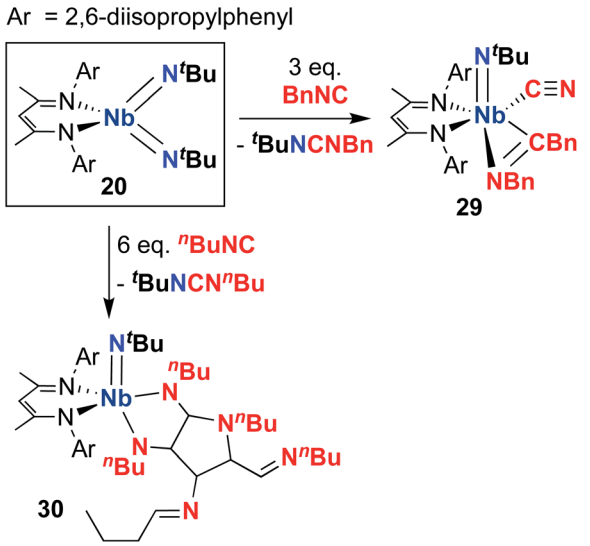

Scheme 10 Reactivity of Nb bis(imido) complex **20** with excess alkyl-substituted isocyanide.

17 reacted with norbornene to give **24**, presumably *via* [2 + 2] cycloaddition to yield an azaniobacyclobutane intermediate. Complex **17** was also observed to react with oxygen-containing unsaturated substrates: addition of (*E*)-4-chloro-chalcone resulted in stereoselective [4 + 2] cycloaddition across the Nb-(*tert*-butyl)imido group to give **25**. Reaction of **17** with *para*-bromo-benzaldehyde resulted in formation of dimeric bis(μ-oxo)-imido **26**, which likely forms *via* a [2 + 2] cycloaddition–cycloreversion sequence.

From 2010–2022, reactivity of BDI-supported Nb bis((*tert*-butyl)imido) **20** was investigated and several synthetic routes to **20** were discovered, as outlined in Scheme 9. Complex **20** can be accessed *via* pyridine abstraction from five-coordinate Nb bis(imido) **27**,[29] or *via* addition of organic azide to MAD-supported bis(imido) **17**,[51] as described above. In 2016, Kriegel *et al.* reported an efficient synthesis for bis(imido) complexes (including **20**, as well as two asymmetric bis(imido) complexes) involving addition of organic azides to low-valent Nb precursor **28**.[57,69] This route proved to be the highest-yielding and cleanest. With an abundant supply of **20** on hand, Arnold, Bergman, and several co-workers proceeded to investigate the remarkable reactivity of this complex.

Complex **20** was observed to mediate catalytic nitrene transfer of alkyl-substituted isocyanides and stoichiometric nitrene metathesis with aryl-substituted isocyanides, as outlined above in Scheme 3, Section 4.1.[57] Complex **20** was also observed to react with three equivalents of benzyl isocyanide to yield **29** (Scheme 10), the product of benzyl group transfer from one isocyanide to another to yield a terminally-bound cyanide ligand and an η^2-iminoacyl group.[57] Remarkably, **20** was observed to react with six equivalents of *n*-butyl isocyanide to yield **30** (Scheme 10); this transformation involves formation of four new C–C bonds and a C–N bond to generate a heavily substituted κ^2-*N*,*N*-pyrrolediamido ligand. To date, this represents the only reported example of such reactivity across the entire transition metal block, highlighting the unique chemistry that can be accessed with group 5 bis(imido) complexes.

Complex **20** was also reported to be active toward 1,2-addition across one of the two Nb-imido double bonds.[30] Exposing a solution of **20** to an H_2 atmosphere established a dynamic equilibrium between **20** and amido-imido-hydrido **31** (Scheme 11). The ratio of **31** to **20** varied based on H_2 pressure, with $K_{eq} \approx 8.0$ at 20 °C under 1 atmosphere of H_2. Placing crystals of **31** under vacuum or exposing a solution of **31** to an N_2 atmosphere resulted in liberation of H_2 and regeneration of bis(imido) **20**. Complex **20** was also observed to react with primary silanes, pinacolborane, *tert*-butylacetylene, and triphenylmethanethiol *via* 1,2-addition across an Nb-imido double bond, resulting in amido-imido products **32-R**, **33**, **34**, and **35**, respectively (Scheme 11). In all cases, the more electronegative substrate fragment was observed to bind to the electropositive Nb center: silanes and boranes resulted in Nb-hydrides, while more acidic substrates led to imido protonation. In the case of amido-imido-thiolate **35**, the BDI ligand binds in a κ^1-fashion, presumably to

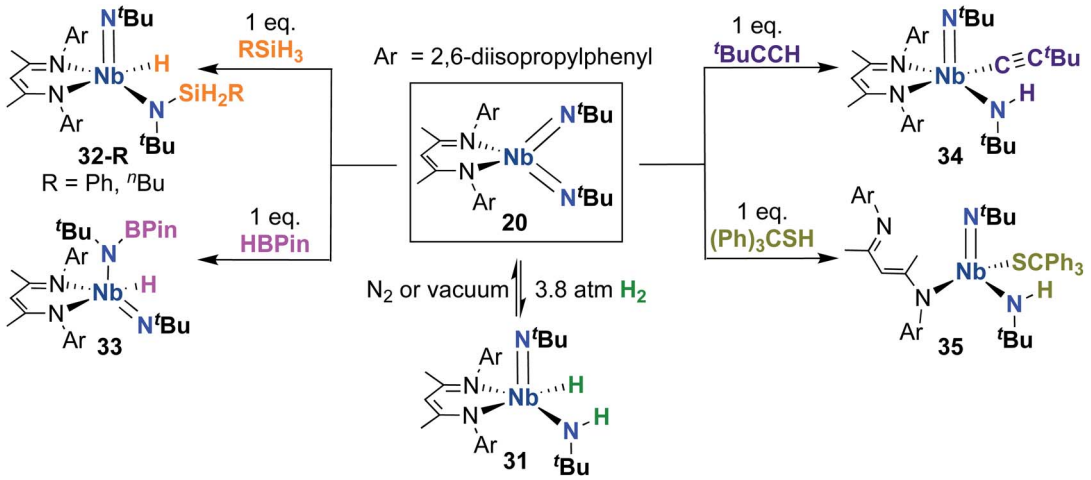

Scheme 11 1,2-Addition reactivity of Nb bis(imido) complex **20** toward element-hydrogen bonds.

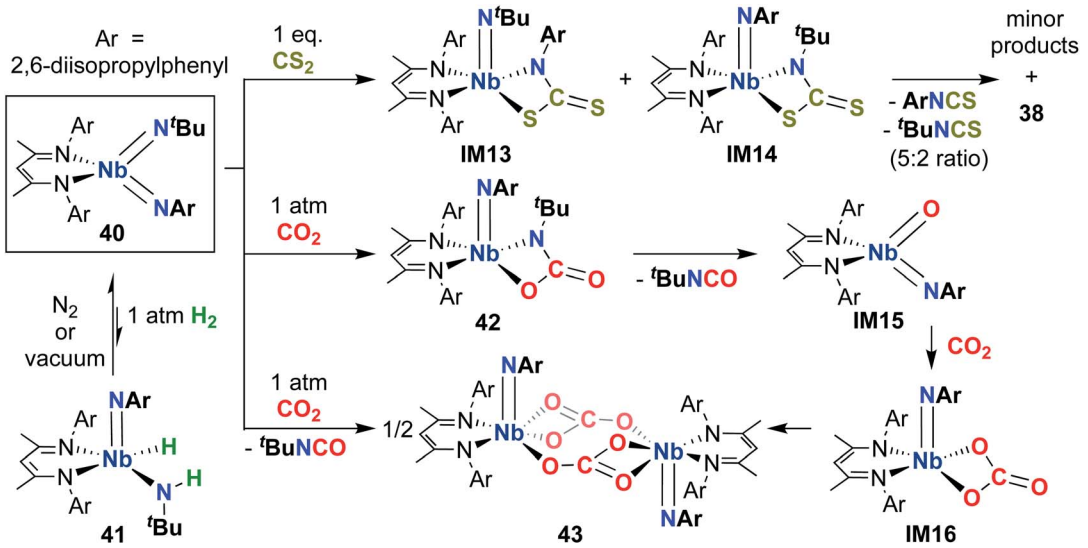

Scheme 12 [2 + 2] Cycloaddition reactivity of Nb bis(imido) complex **20** toward heteroallenes.

relieve steric clash with the triphenylmethanethiolato ligand. The related mono(imido) complexes (BDI)Nb(N^{t}Bu)Cl$_2$ and (BDI)Nb(N^{t}Bu)F$_2$ were not observed to react with H_2, silanes, boranes, acetylene, or thiols,[29] suggesting that π-loading enhances reactivity at imido groups in this system.

Building on the 1,2-addition and metathesis reactivity described above, **20** was also found to be capable of mediating [2 + 2] cycloadditions of heteroallenes across one of the two Nb-imido bonds.[29,30] Complex **20** was observed to undergo [2 + 2] cycloaddition with *tert*-butyl isocyanate[29] and diphenylketene[30] to yield oxaazaniobacyclobutane products **36** and **37**, respectively (Scheme 12). Complex **36** was found to decompose readily in solution to liberate carbodiimide, while **37** was stable in solution at room temperature and liberated diphenylethenimine upon heating. The related reactions of **20** with CS_2 or CO_2 led instead to dimeric products **38** and **39**, respectively (Scheme

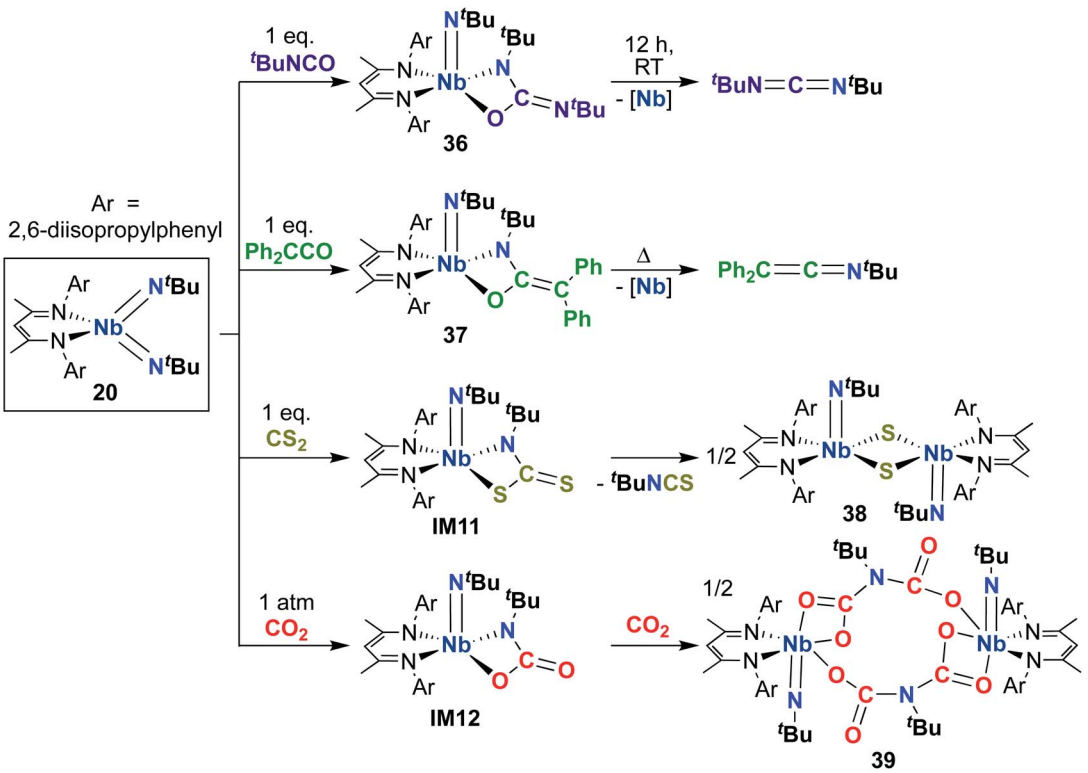

Scheme 13 1,2-Addition and [2 + 2] cycloaddition reactivity of asymmetric Nb bis(imido) complex **40**.

12).[30] Reaction with CS_2 presumably occurs *via* initial [2 + 2] cycloaddition to generate sulfaazaniobacyclobutane intermediate **IM11**, which proceeds to liberate isothiocyanate *via* a retro-[2 + 2] process and generate a transient imido–sulfido species, which dimerizes to give the bis(μ-sulfido)-imido product. Similarly, reaction with CO_2 also likely forms oxaazaniobacyclobutane intermediate **IM12** *via* [2 + 2] cycloaddition; this species then inserts another equivalent of CO_2 into the metallacycle before dimerizing, suggesting that insertion of CO_2 occurs more rapidly than retrocycloaddition in this case. These reactions showcase the highly reactive nature of π-loaded bis(imido) complexes and highlight the driving force provided by formation of strong Nb-oxo bonds.

What factors, aside from π-loading, contribute to the significant reactivity of symmetric bis(imido) **20**? Comparison of reactivity patterns between **20** and asymmetric bis(imido) **40** provides answers (Scheme 13).[70] First, **40** was observed to be far less reactive toward 1,2-addition: addition of H_2 resulted in low conversion to amido-imido-hydrido product **41**, with $K_{eq} \approx 2.5$ at 20 °C under 1 atmosphere of H_2 ($K_{eq} \approx 8.0$ for symmetric bis(imido) **20**). 1,2-Addition of H_2 occurred solely across the Nb-(*tert*-butyl)imido bond. Complex **40** reacted sluggishly with other 1,2-addition substrates (silanes, boranes, thiols); these reactions were not pursued further. The authors suggested that the weakly electron withdrawing nature of the 2,6-diisopropylphenyl group serves to stabilize the Nb=NAr bonding interaction, while the weakly electron donating *tert*-butyl moiety increases electron density at the imido group, leading to heightened reactivity at the Nb=N^{t}Bu bond. These subtle electronic factors also come into play when comparing reactivity patterns of bis((*tert*-butyl))imido) **20** with (*tert*-butyl)imido-(aryl) imido **40**. As such, π-loading can be fine-tuned by choice of imido group substituent, with electron donating alkyl groups leading to more reactive bis(imido) complexes.

Complex **40** was also observed to react with heteroallenes across one of the two Nb-imido bonds: addition of CO_2 led to oxaazaniobacycle **42** (Scheme 13), the product of [2 + 2] cycloaddition across the Nb-(*tert*-butyl)imido bond.[30] Complex **42** was observed to undergo retro-cycloaddition in solution under an atmosphere of CO_2 to release isocyanate, yielding the four-coordinate oxo-imido intermediate **IM15**. This intermediate can insert another equivalent of CO_2 to yield carbonate intermediate **IM16**, which dimerizes to yield the observed carbonate-bridged product **43**. Surprisingly, **40** was found to react with CS_2 across both the (*tert*-butyl)imido and (aryl)imido groups, yielding bis(μ-sulfido)-imido dimer **38**, a 5 : 2 mixture of aryl- and (*tert*-butyl)-isothiocyanate, and a mixture of minor side products. This reaction was proposed to proceed through sulfaazaniobacyclobutane intermediates **IM13** and **IM14**; the observed reactivity across the (aryl)imido group was attributed to increased steric bulk, which prevents dimerization to form a stable bis(μ-sulfido)-(aryl)imido product akin to **38**.

Indeed, observed reactivity of the (BDI) Nb bis(imido) system appears to be quite sensitive to imido group steric profile. As

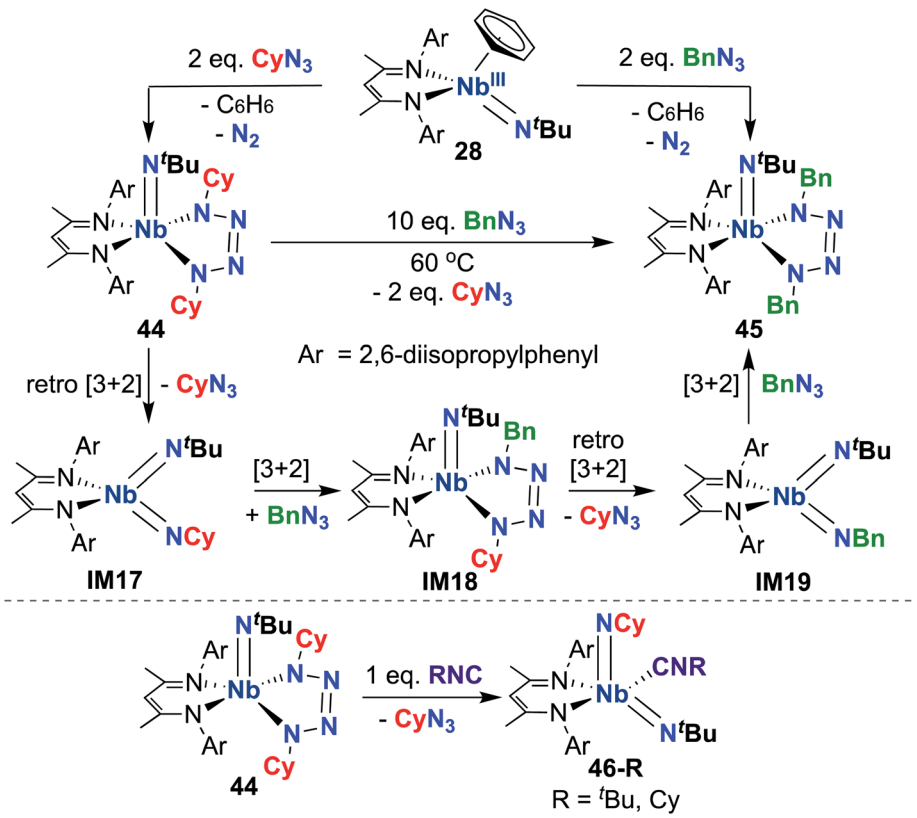

Scheme 14 [3 + 2] Cycloaddition and retro-cycloaddition reactivity of Nb tetrazene complexes.

mentioned previously, several bis(imido) complexes can be accessed *via* reaction of low-valent Nb mono(imido) precursor **28** with organic azides (Scheme 9), including bis((*tert*-butyl)) imido) (**20**), (*tert*-butyl)imido-(2,6-diisopropylphenyl)imido (**40**), and (*tert*-butyl)imido-(trimethylsilyl)imido.[57] However, when less sterically demanding substituents are employed, such as cyclohexyl or benzyl, mono(imido) tetrazene complexes are instead isolated (**44** and **45**, respectively; Scheme 14, top).[67] These complexes were hypothesized to form from initial nitrene transfer to yield unstable four-coordinate bis(imido) intermediates **IM17** and **IM19**, followed by [3 + 2] cycloaddition of a second equivalent of azide. Cyclohexyl derivative **44** was observed to undergo azide metathesis to form benzyl derivative **45**; experimental and computational investigations support a mechanism in which bis(imido) intermediates **IM17** and **IM19** are formed *via* retro-[3 + 2]-cycloaddition from tetrazene complex **44** and spectroscopically observed tetrazene intermediate **IM18**, respectively. Notably, bis(imido) intermediate **IM17** could be trapped upon addition of a bulky Lewis base to yield stable five-coordinate bis(imido) complexes **46-R** (R = *tert*-butyl, cyclohexyl; Scheme 14, bottom).

The chemistry of Bergman and Arnold's (BDI)Nb bis(imido) system has been explored extensively, leading to the emergence of several themes. First, π-loading *via* addition of a second imido group makes bis(imido) complexes reactive toward nitrene transfer, 1,2-addition, and overall [2 + 2], [2 + 4], and [3 + 2] cycloadditions; in contrast, related mono(imido) systems do not display these reactivity patterns. Second, reactivity of bis(imido) complexes can be tuned by choice of imido substituent, with electron-donating groups leading to weaker Nb–N_{imido} bonding interactions and enhanced reactivity. Finally, bulky R-groups at BDI and imido ligands serve to kinetically stabilize reactive four-coordinate bis(imido) complexes. These guiding principles can be used to inform the design of bis(imido) complexes of vanadium, tantalum, and of other metals of the early transition metal block.

4.2.3. Stoichiometric reactivity of tantalum bis(imido) complexes. In 1993, Schaller and Wolczanski reported the first example of reactivity mediated by a π-loaded Ta bis(imido) complex.[39] Upon heating, the mono(imido) Ta complexes **47-R** (R = Me, Ph; Scheme 15, top) were observed to liberate methane or benzene *via* reductive elimination to yield unstable bis(imido) intermediate **IM20**. This intermediate was observed to exist in dynamic equilibrium with **47-R**, indicating that this bis(imido) species is capable of activating the strong C–H bonds of methane and benzene. Bis(imido) intermediate **IM20** was observed to react with another equivalent of starting material **47-Ph** *via* C–H activation of the *para*-position of the bound phenyl ligand, yielding benzene-bridged **48**. When thermolysis was carried out in C_6D_6, conversion to deuterated derivatives **49-d_1** and **49-d_2** was observed. These complexes likely formed *via* C–D activation across a Ta-imido group, leading to a mono(imido) complex with a C_6D_5 ligand and two amido groups. Finally, thermolysis of **47-Me** led to pyridine-stabilized bis(imido) **50** *via* reductive elimination of methane; isolation of **50** provides support for the identities of proposed bis(imido) intermediates **IM20** and **IM21**.

A report from Royo and Sánchez-Nieves in 2000 represents the second and final example of a reactive of Ta bis(imido) complex.[27] Mono(imido) **51** (Scheme 15, bottom) was observed to yield mono(imido) complexes **52-R** (R = C_6H_5, C_6H_4Me) upon thermolysis in benzene or toluene solvent. Based on literature precedent,[39] it seems likely that this transformation proceeds *via* reductive elimination of methane to yield π-loaded bis(imido) intermediate **IM22**, which can activate aromatic C–H bonds across one of the two Ta-imido groups. However, since no

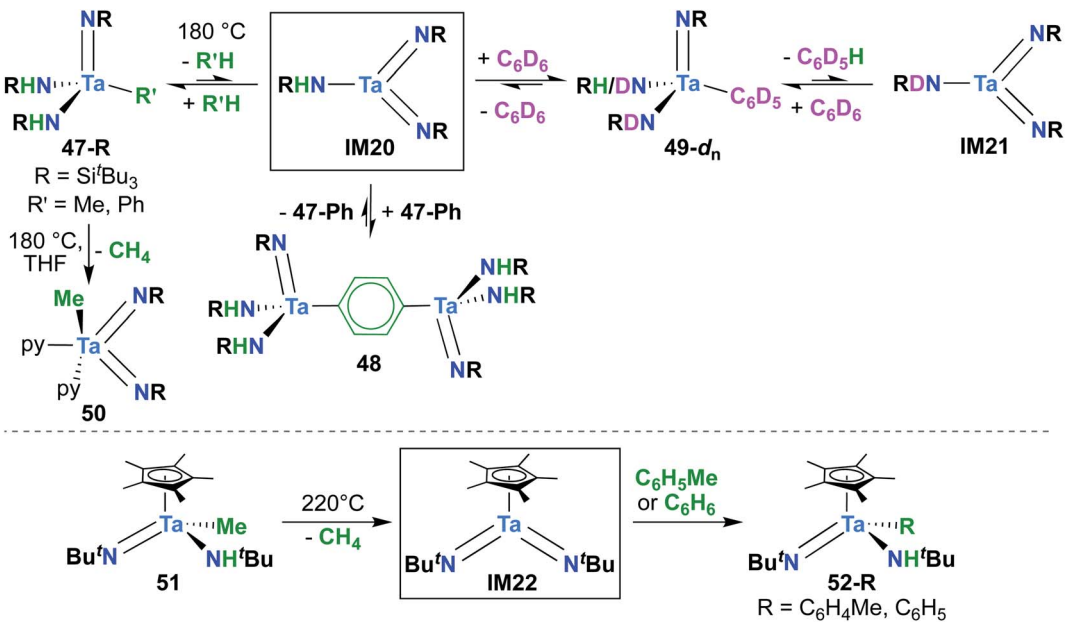

Scheme 15 C–H activation reactivity of transient Ta bis(imido) complexes.

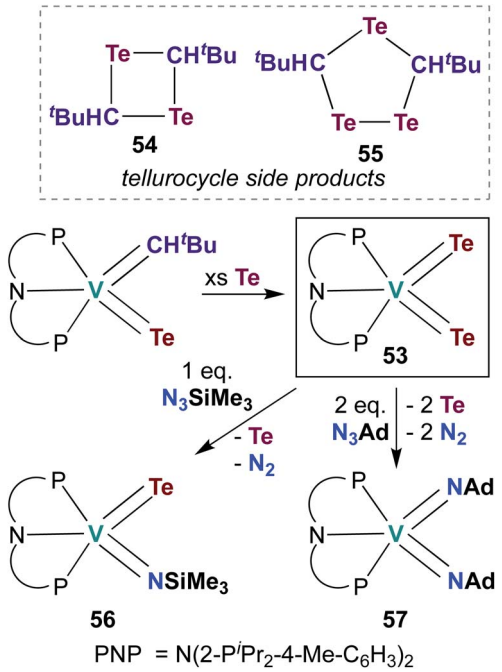

Scheme 16 Synthesis and reactivity of V bis(tellurido) complex **53**.

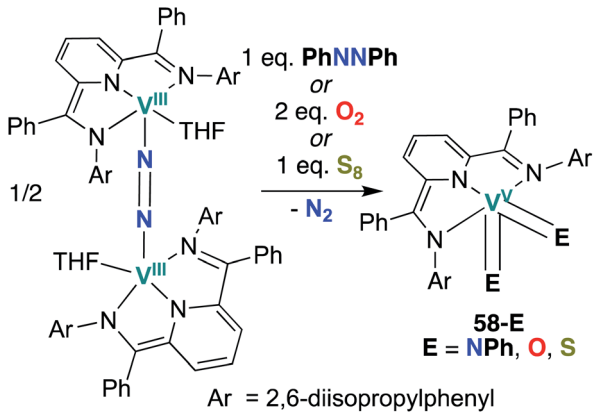

Scheme 17 Syntheses of V bis(imido), bis(oxo), and bis(sulfido) complexes **58-E**.

isotope labelling studies were carried out and **IM22** could not be trapped, a simple σ-bond metathesis mechanism cannot be ruled out.[64]

5. Synthesis and reactivity of π-loaded chalcogenido complexes

The examples of catalytic and stoichiometric bis(imido) reactivity given above provide support for the claim that π-loading leads to increased reactivity at group 5 metal–imido linkages. A few researchers have begun to extend this strategy toward d^0 group 5 chalcogenido–imido and bis(chalcogenido) complexes, which are isolobal to the bis(imido) complexes discussed above. This emerging field of research has already led to new types of complexes and new modes of reactivity for the early transition metals.

In 2009, Mindiola and co-workers reported V bis(tellurido) **53** (Scheme 16), the first example of such a complex in the group 5 transition metal literature.[71] A crystal structure of **53** supported assignment a V(v) metal center, as the intramolecular Te–Te distance was observed to be too long for an η^2-Te_2^{2-}-type ligand bound to a V(iii) metal center. However, the V–Te bond lengths in **53** were found to be shorter than a corresponding mono(tellurido) complex;[71] these bond metrics are inconsistent with the π-loading hypothesis. Synthesis of **53** also resulted in formation of ditelluretane **54** and tritellurolane **55**. Bis(tellurido) **53** was found to react with one or two equivalents of organic azide to yield tellurido-imido **56** and bis(imido) **57**, respectively. Unfortunately, a crystal structure of tellurido-imido **56** was not obtained, nor was reactivity reported, so the presence or extent of π-loading in this complex cannot be evaluated. The authors hypothesized that reaction of **53** with organic azides proceeds *via* elimination of Te^0 to form a transient V(iii) complex, as opposed to mechanism involving [2 + 2] cycloaddition. Thus, it appears that V bis(tellurido) complexes are not strictly analogous to π-loaded V bis(imido) complexes (although the nature of tellurido–imido complexes remains an open question).

Chirik and co-workers reported two more examples of V bis(chalcogenido) complexes in 2012: bis(imido), bis(oxo), and

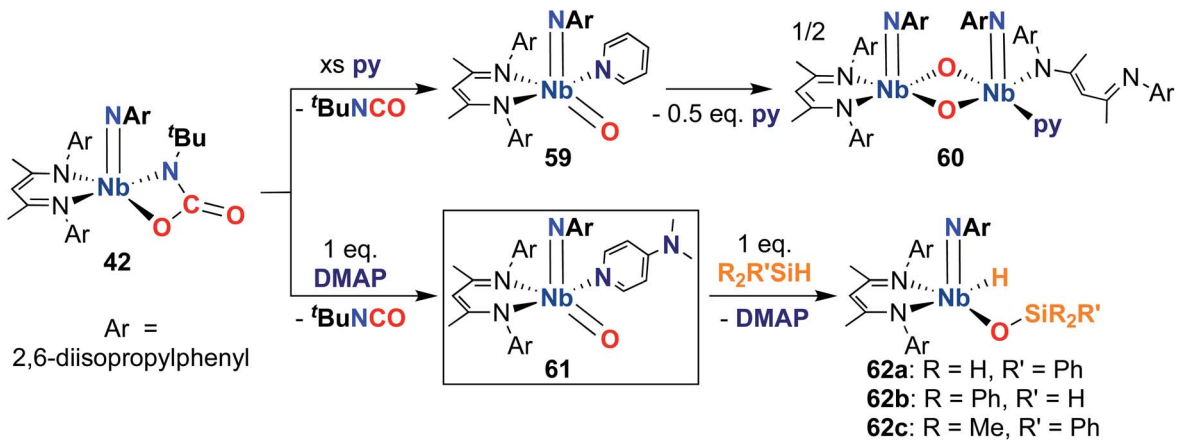

Scheme 18 Synthesis and 1,2-addition reactivity of π-loaded Nb oxo-imido complex **61**.

bis(sulfido) complexes **58-E** (E = NPh, O, S; Scheme 17) were synthesized from a dinitrogen-bridged V(III) precursor.[56] Bond metrics in complexes **58-O** and **58-S** cannot be compared to analogous mono(chalcogenido) complexes to evaluate the extent of π-loading, as such complexes have not been reported. Similarly, reactivity of complexes **58-O** and **58-S** has not yet been reported.

Finally, in 2020, Bergman, Arnold, and co-workers reported the synthesis of a reactive, π-loaded oxo-imido complex.[30] As described earlier, imido-oxaazaniobacycle **42** can be accessed from bis(imido) **40** (Scheme 13); addition of Lewis bases to **42** resulted in expulsion of isocyanate to yield five-coordinate oxo–imido complexes **59** and **61** (Scheme 18). The pyridine derivative **59** was found to be unstable in solution, liberating half an equivalent of pyridine and dimerizing to give bis(μ-oxo)-imido dimer **60**, which was observed to be quite unreactive. However, the 4-dimethylaminopyridne derivative **61** was more stable than **59**, enabling a crystal structure of this complex to be obtained; this represents the only structurally characterized group 5 terminal oxo-imido complex reported to date. The bond metrics in this structure were found to be consistent with a π-loaded complex, as detailed in Section 2. Complex **61** was found to react with primary, secondary, and tertiary silanes across the Nb-oxo bond *via* 1,2-addition to yield complexes **62a–c**. 1,2-Addition reactions across group 5-oxo complexes are rare,[72] and to date, no other examples of such reactivity have been reported for Nb-oxo complexes.[73] In the case of **61**, it's clear that π-loading contributes to polarizing the Nb-oxo group, engendering reactivity at a group that usually spectates. This result suggests that the π-loading strategy can be extended to chalcogenido–imido complexes, enabling new modes of reactivity for these complexes.

6. Conclusions and future outlook

The above examples illustrate instances in which imido-based reactivity is observed in π-loaded bis(imido) complexes of the group 5 triad. While there are numerous examples of such reactivity reported for bis(imido) complexes, there are far fewer examples of mono(imido)-mediated reactivity, suggesting that π-loading activates group 5-imidos towards reactivity. Of the examples presented above, catalysis is dominated by V bis(imido) complexes supported by labile and relatively unbulky ligands, while Nb bis(imido) complexes supported by bulky bidentate ligands represent the most stoichiometrically active species. In general, the stoichiometric reactivity of V and Ta bis(imido) complexes is underexplored, as is the chemistry of Nb bis(imido) systems supported by ligands other than BDI and MAD.

In terms of catalysis, it seems likely that labile ligands (*i.e.*, PR_3, THF, py), less steric bulk at ancillary ligand(s), and cationic charge could lead to more examples of V- and Nb-mediated catalytic processes. Ta systems are particularly underexplored: to date, only three structurally characterized examples of Ta bis(imido) complexes have been reported. It seems likely that bulky ancillary ligands will be needed to stabilize Ta bis(imido) species, as the few examples of such complexes reported to date are highly reactive and often transient. Notably, verified examples of cycloadditions across imido groups of Ta bis(imido) complexes are absent from the literature (although it seems likely that [2 + 2] cycloaddition occurs along Hollis' catalytic cycle[32]).

Chalcogenido–imido and reactive bis(chalcogenido) species are underexplored for all metals of the group 5 triad. Promising results with a reactive Nb oxo-imido species suggest that the π-loading strategy can be extended towards this class of complexes. The synthesis and study of group 5 terminal oxo-imido, sulfido-imido, and bis(chalcogenido) species is an open field, and one that will surely lead to interesting chemistry.

The rational design of highly reactive, π-loaded group 5 complexes will lead to systems capable of mediating challenging transformations with implications for a sustainable chemical future. Desirable transformations include N–H bond activation of ammonia, C–H bond activation of methane, conversion of CO_2 into larger C_n products (such as isocyanates and carbamates, as described above for niobium bis(imido) complexes), and synthesis of higher-value cyclic and linear hydrocarbons from plentiful feedstock molecules. Employing relatively abundant and affordable early transition metals to carry out these transformations will help ameliorate the overuse of expensive precious metal catalysts, and ultimately contribute to a greener chemical industry.

Author contributions

J. I. F. conceived and wrote the manuscript. J. M., S. L.-F., and D. A. contributed to schemes and figures. R. G. B. and J. A. conceived and contributed to all portions of the manuscript.

Conflicts of interest

There are no conflicts to declare.

Note added after first publication

This version replaces the manuscript published on 29th June 2022. The images of Schemes 4–7 had been associated with the incorrect captions and were out of order. The RSC apologises for any confusion.

Acknowledgements

This work was funded by the NSF (Grant No. CHE-1465188 and 1954612 to J. A. and R. G. B.). J. I. F. acknowledges support from an NSF graduate research fellowship (Grant No. DGE 1752814). We thank Dr Michael A. Boreen, Erik T. Ouellette, I. Joseph Brackbill, Sheridon N. Kelly, and Anukta Jain for helpful discussions.

Notes and references

1 D. E. Wigley, in *Progress in Inorganic Chemistry*, ed. K. D. Karlin, John Wiley & Sons, Inc., 1994, pp. 239–482.

2 K. Kawakita, B. F. Parker, Y. Kakiuchi, H. Tsurugi, K. Mashima, J. Arnold and I. A. Tonks, *Coord. Chem. Rev.*, 2020, **407**, 213118–213141.
3 J. R. Webb, S. A. Burgess, T. R. Cundari and T. B. Gunnoe, *Dalton Trans.*, 2013, **42**, 16646–16665.
4 P. T. Wolczanski, *Organometallics*, 2018, **37**, 505–516.
5 J. Chu, E. Lu, Y. Chen and X. Leng, *Organometallics*, 2013, **32**, 1137–1140.
6 A. P. Duncan and R. G. Bergman, *Chem. Rec.*, 2002, **2**, 431–445.
7 J. Chu, X. Han, C. E. Kefalidis, J. Zhou, L. Maron, X. Leng and Y. Chen, *J. Am. Chem. Soc.*, 2014, **136**, 10894–10897.
8 A. F. Heyduk, R. A. Zarkesh and A. I. Nguyen, *Inorg. Chem.*, 2011, **50**, 9849–9863.
9 P. J. Walsh, F. J. Hollander and R. G. Bergman, *J. Am. Chem. Soc.*, 1988, **110**, 8729–8731.
10 C. C. Cummins, S. M. Baxter and P. T. Wolczanski, *J. Am. Chem. Soc.*, 1988, **110**, 8731–8733.
11 J. Chu, E. Lu, Z. Liu, Y. Chen, X. Leng and H. Song, *Angew. Chem., Int. Ed.*, 2011, **50**, 7677–7680.
12 N. Hazari and P. Mountford, *Acc. Chem. Res.*, 2005, **38**, 839–849.
13 S. W. Krska, R. L. Zuckerman and R. G. Bergman, *J. Am. Chem. Soc.*, 1998, **120**, 11828–11829.
14 K. E. Meyer, P. J. Walsh and R. G. Bergman, *J. Am. Chem. Soc.*, 1994, **116**, 2669–2670.
15 Y. Li, Y. Shi and A. L. Odom, *J. Am. Chem. Soc.*, 2004, **126**, 1794–1803.
16 A. L. Odom and T. J. McDaniel, *Acc. Chem. Res.*, 2015, **48**, 2822–2833.
17 R. T. Ruck, R. L. Zuckerman, S. W. Krska and R. G. Bergman, *Angew. Chem., Int. Ed.*, 2004, **43**, 5372–5374.
18 F. Basuli, H. Aneetha, J. C. Huffman and D. J. Mindiola, *J. Am. Chem. Soc.*, 2005, **127**, 17992–17993.
19 Z. W. Davis-Gilbert, L. J. Yao and I. A. Tonks, *J. Am. Chem. Soc.*, 2016, **138**, 14570–14573.
20 Z. W. Gilbert, R. J. Hue and I. A. Tonks, *Nat. Chem.*, 2016, **8**, 63–68.
21 E. P. Beaumier, M. E. McGreal, A. R. Pancoast, R. H. Wilson, J. T. Moore, B. J. Graziano, J. D. Goodpaster and I. A. Tonks, *ACS Catal.*, 2019, **9**, 11753–11762.
22 A. J. Pearce, R. P. Harkins, B. R. Reiner, A. C. Wotal, R. J. Dunscomb and I. A. Tonks, *J. Am. Chem. Soc.*, 2020, **142**, 4390–4399.
23 A. I. Nguyen, R. A. Zarkesh, D. C. Lacy, M. K. Thorson and A. F. Heyduk, *Chem. Sci.*, 2011, **2**, 166–189.
24 M. C. Burland, T. W. Pontz and T. Y. Meyer, *Organometallics*, 2002, **21**, 1933–1941.
25 R. E. Blake, D. M. Antonelli, L. M. Henling, W. P. Schaefer, K. I. Hardcastle and J. E. Bercaw, *Organometallics*, 1998, **17**, 718–725.
26 S. M. Rocklage and R. R. Schrock, *J. Am. Chem. Soc.*, 1980, **102**, 7809–7811.
27 P. Royo and J. Sánchez-Nieves, *J. Organomet. Chem.*, 2000, **597**, 61–68.
28 J. W. Bruno and X. J. Li, *Organometallics*, 2000, **19**, 4672–4674.
29 N. C. Tomson, J. Arnold and R. G. Bergman, *Organometallics*, 2010, **29**, 2926–2942.
30 J. I. Fostvedt, L. N. Grant, B. M. Kriegel, A. H. Obenhuber, T. D. Lohrey, R. G. Bergman and J. Arnold, *Chem. Sci.*, 2020, **11**, 11613–11632.
31 D. P. Smith, K. D. Allen, M. D. Carducci and D. E. Wigley, *Inorg. Chem.*, 1992, **31**, 1319–1320.
32 T. R. Helgert, X. Zhang, H. K. Box, J. A. Denny, H. U. Valle, A. G. Oliver, G. Akurathi, C. E. Webster and T. K. Hollis, *Organometallics*, 2016, **35**, 3452–3460.
33 A. M. Baranger, P. J. Walsh and R. G. Bergman, *J. Am. Chem. Soc.*, 1993, **115**, 2753–2763.
34 G. Parkin, L. R. Whinnery, A. van Asselt, D. J. Leahy, N. G. Hua, R. W. Quan, L. M. Henling, W. P. Schaefer, B. D. Santarsiero and J. E. Bercaw, *Inorg. Chem.*, 1992, **31**, 82–85.
35 D. N. Huh, Y. Cheng, C. W. Frye, D. T. Egger and I. A. Tonks, *Chem. Sci.*, 2021, **12**, 9574–9590.
36 P. D. Bolton and P. Mountford, *Adv. Synth. Catal.*, 2005, **347**, 355–366.
37 P. A. Zhizhko, N. S. Bushkov, A. V. Pichugov and D. N. Zarubin, *Coord. Chem. Rev.*, 2021, **448**, 214112.
38 D. S. Williams, M. H. Schofield and R. R. Schrock, *Organometallics*, 1993, **12**, 4560–4571.
39 C. P. Schaller and P. T. Wolczanski, *Inorg. Chem.*, 1993, **32**, 131–144.
40 H. S. La Pierre, J. Arnold, R. G. Bergman and F. D. Toste, *Inorg. Chem.*, 2012, **51**, 13334–13344.
41 H. S. La Pierre, S. G. Minasian, M. Abubekerov, S. A. Kozimor, D. K. Shuh, T. Tyliszczak, J. Arnold, R. G. Bergman and F. D. Toste, *Inorg. Chem.*, 2013, **52**, 11650–11660.
42 D. Rehder, T. Polenova and M. Bühl, *Annu. Rep. NMR Spectrosc.*, 2007, **62**, 49–114.
43 D. Rehder, *Coord. Chem. Rev.*, 2008, **252**, 2209–2223.
44 F. Preuss, T. Wieland and B. Günther, *Z. Anorg. Allg. Chem.*, 1992, **609**, 45–50.
45 F. Preuss, H. Becker and T. Weiland, *Z. Naturforsch.*, 1990, **45b**, 191–198.
46 K. M. Lin, P. Y. Wang, Y. J. Shieh, H. Z. Chen, T. S. Kuo and Y. C. Tsai, *New J. Chem.*, 2010, **34**, 1737–1745.
47 H. S. La Pierre, J. Arnold and F. D. Toste, *Angew. Chem., Int. Ed.*, 2011, **50**, 3900–3903.
48 K. Kawakita, E. P. Beaumier, Y. Kakiuchi, H. Tsurugi, I. A. Tonks and K. Mashima, *J. Am. Chem. Soc.*, 2019, **141**, 4194–4198.
49 W. S. Farrell, C. Greene, P. Ghosh, T. H. Warren and P. Y. Zavalij, *Organometallics*, 2020, **39**, 3906–3917.
50 B. L. Tran, M. Singhal, H. Park, O. P. Lam, M. Pink, J. Krzystek, A. Ozarowski, J. Telser, K. Meyer and D. J. Mindiola, *Angew. Chem., Int. Ed.*, 2010, **49**, 9871–9875.
51 A. H. Obenhuber, T. L. Gianetti, X. Berrebi, R. G. Bergman and J. Arnold, *J. Am. Chem. Soc.*, 2014, **136**, 2994–2997.
52 T. R. Helgert, T. K. Hollis, A. G. Oliver, H. U. Valle, Y. Wu and C. E. Webster, *Organometallics*, 2014, **33**, 952–958.
53 Y.-W. Chao, P. A. Wexler and D. E. Wigley, *Inorg. Chem.*, 1990, **29**, 4594–4595.

54 Y.-W. Chao, P. A. Wexler and D. E. Wigley, *Inorg. Chem.*, 1989, **28**, 3860–3868.
55 Y. Tsai, P. Wang, K. Lin, S. Chen and J. Chen, *Chem. Commun.*, 2008, **2008**, 205–207.
56 C. Milsmann, Z. R. Turner, S. P. Semproni and P. J. Chirik, *Angew. Chem., Int. Ed.*, 2012, **51**, 5386–5390.
57 B. M. Kriegel, R. G. Bergman and J. Arnold, *J. Am. Chem. Soc.*, 2016, **138**, 52–55.
58 N. C. Tomson, J. Arnold and R. G. Bergman, *Organometallics*, 2010, **29**, 5010–5025.
59 J. de With, A. D. Horton and A. G. Orpen, *Organometallics*, 1993, **12**, 1493–1496.
60 S. G. Bott, D. M. Hoffman and S. P. Rangarajan, *Inorg. Chem.*, 1995, **34**, 4305–4310.
61 E. P. Beaumier, A. J. Pearce, X. Y. See and I. A. Tonks, *Nat. Rev. Chem*, 2019, **3**, 15–34.
62 T. Saito, H. Nishiyama, H. Tanahashi, K. Kawakita, H. Tsurugi and K. Mashima, *J. Am. Chem. Soc.*, 2014, **136**, 5161–5170.
63 G. Liang, T. K. Hollis and C. E. Webster, *Organometallics*, 2018, **37**, 1671–1681.
64 J. de With and A. D. Horton, *Angew. Chem., Int. Ed.*, 1993, **32**, 903–905.
65 T. Gehrmann, J. Lloret Fillol, H. Wadepohl and L. H. Gade, *Organometallics*, 2012, **31**, 4504–4515.
66 K. E. Meyer, P. J. Walsh and R. G. Bergman, *J. Am. Chem. Soc.*, 1995, **117**, 974–985.
67 A. Jain, J. I. Fostvedt, B. M. Kriegel, D. W. Small, L. N. Grant, R. G. Bergman and J. Arnold, *Inorg. Chem.*, 2022, **61**, 6574–6583.
68 A. H. Obenhuber, T. L. Gianetti, R. G. Bergman and J. Arnold, *Chem. Commun.*, 2015, **51**, 1278–1281.
69 T. L. Gianetti, G. Nocton, S. G. Minasian, N. C. Tomson, A. L. D. Kilcoyne, S. A. Kozimor, D. K. Shuh, T. Tyliszczak, R. G. Bergman and J. Arnold, *J. Am. Chem. Soc.*, 2013, **135**, 3224–3236.
70 B. M. Kriegel, R. G. Bergman and J. Arnold, *J. Am. Chem. Soc.*, 2016, **138**, 52–55.
71 U. J. Kilgore, J. A. Karty, M. Pink, X. Gao and D. J. Mindiola, *Angew. Chem., Int. Ed.*, 2009, **48**, 2394–2397.
72 J. I. Fostvedt, M. A. Boreen, R. G. Bergman and J. Arnold, *Inorg. Chem.*, 2021, **60**, 9912–9931.
73 G. Parkin, in *Progress in Inorganic Chemistry*, ed. K. D. Karlin, John Wiley & Sons, Inc., 1998, pp. 1–165.